



# 1 **Machine-learning approach to crop yield prediction with the spatial** 2 **extent of drought**

3 Vitali Diaz<sup>1,2</sup>, Ahmed A.A. Osman<sup>3</sup>, Gerald A. Corzo Perez<sup>1,2</sup>, Henny A.J. Van Lanen<sup>4</sup>,  
4 Shreedhar Maskey<sup>2</sup>, Dimitri Solomatine<sup>1,2,5</sup>

5 <sup>1</sup>IHE Delft Institute for Water Education, Hydroinformatics Chair group, Delft, 2601 DA, the Netherlands

6 <sup>2</sup>Delft University of Technology, Delft, the Netherlands

7 <sup>3</sup>Arcadis, Wales, United Kingdom

8 <sup>4</sup>Hydrology and Quantitative Water Management Group, Wageningen University, Wageningen, the Netherlands

9 <sup>5</sup>Water Problems Institute of the Russian Academy of Sciences, Moscow, Russia

10 **Corresponding author:** Vitali Diaz; v.diazmercado@tudelft.nl; vitalidime@gmail.com

## 11 **Abstract**

12 Crop yield is one of the variables used to assess the impact of droughts on agriculture. Crop growth  
13 models calculate yield and variables related to plant development and become more suitable for crop  
14 yield estimation. However, these models are limited in that specific data are needed for computation.  
15 Given this limitation, machine learning (ML) models are often widely utilised instead, but their use  
16 with the spatial characteristics of droughts as input data is limited. This research explored the spatial  
17 extent of drought (area) as input data for building an approach to predict seasonal crop yield. This ML  
18 approach is made up of two components. The first includes polynomial regression (PR) models, and the  
19 second considers artificial neural network (ANN) models. In this approach, the purpose was to evaluate  
20 both types of ML models (PR and ANN) and integrate them into one operational tool. The logic is as  
21 follows: ANN models determine the most accurate predictions, but in practice, issues regarding data  
22 retrieval and processing can make the use of equations, i.e. PR, preferable. The proposed approach  
23 provides these PR equations to perform such calculations with early and preliminary input. The  
24 estimates can be further improved when the ANN models are run with the final input data. The results  
25 indicated that the empirical equations (PR) produced good predictions when using drought area as the  
26 input. ANN provides better estimates, in general. This research will improve drought monitoring  
27 systems for assessing drought effects. Since it is currently possible to calculate drought areas within  
28 these systems, the direct application of the prediction of drought effects is possible to integrate by  
29 following approaches such as the one presented or similar.

## 30 **Keywords**

31 Spatio-temporal analysis, crop yield, drought impact, machine learning, agricultural drought

## 32 **1 Introduction**

33 Drought continually hits many regions across the world. It negatively affects various human  
34 activities such as agriculture, which not only generates economic losses but can also trigger



35 famine, causing millions of deaths (Below et al., 2007; Food and Agriculture Organization of  
36 the United Nations (FAO), 2017; Kim et al., 2019; Sheffield and Wood, 2011; World  
37 Meteorological Organization (WMO), 2006). Hence, methods that help to improve strategies  
38 for drought mitigation are necessary. Within these methods are those that allow predicting the  
39 impacts of drought.

40 Assessments of drought impacts confirm that the presence of drought on human activities can  
41 be devastating. For instance, the Food and Agriculture Organization of the United Nations  
42 (FAO) calculated the damage and losses in the agricultural sector caused by five types of  
43 hazards, including drought. FAO estimates that drought causes damages and losses to this  
44 sector by up to 80% (FAO, 2017). Although multiple factors are involved in agriculture  
45 affectation, drought often plays the primary role, as literature confirms (Dai, 2011; FAO, 2017;  
46 Kim et al., 2019).

47 The assessment of drought impacts on agriculture can be performed in terms of crop yield.  
48 FAO defines crop yield as the measure of the yield of a crop per unit area of land cultivation  
49 (in kg/ha or ton/ha) (FAO and DWFI, 2015). For assessing crop yield under drought affectation,  
50 physical models based on crop properties turn out to be more comprehensive and descriptive  
51 (Huang et al., 2019; Reynolds et al., 2000; White et al., 1997; Wu et al., 2016). However, an  
52 important barrier to such models' realisation is the lack of detailed crop data and the difficulty  
53 representing all the processes involved in all stages of crop development (Huang et al., 2019;  
54 Reynolds et al., 2000; Wu et al., 2016).

55 Statistical and machine-learning (ML) models, which involve mathematical equations to  
56 calculate the output of a model with suitable input(s), can be used to assess crop yield impact  
57 by drought without considering any biological or physical process of the crop but the analysis  
58 of the input and output data (Chlingaryan et al., 2018; Rahmati et al., 2020; Udmale et al.,  
59 2020; van Klompenburg et al., 2020). There have been studies where various inputs, ML  
60 techniques and architectures (configurations) have been tested for crop yield prediction (e.g.,  
61 Chlingaryan et al., 2018; van Klompenburg et al., 2020). However, the spatial extent of drought  
62 (area) is an input that has not been fully explored previously to crop yield prediction. The  
63 prediction refers to the calculation of crop yield at the end of the growing season (harvesting)  
64 with information available before or during the crop development season (pre-harvesting).

65 This research aims to develop an ML approach to calculate seasonal crop yield (CY) with the  
66 monthly drought areas (DAs) as input. The ML approach comprises two components. Each  
67 component includes a set of the following types of ML models: polynomial regression (PR)  
68 and artificial neural network (ANN). The goal is to build both types of ML models (ANN and



69 MR) and use them as an integrated tool to support the decisions made based on crop yield  
70 prediction. The logic is as follows. PR provides the prediction where the crop yield calculation  
71 is "clear" to the performer (the end-user) because she/he has access to the equations that have  
72 a straightforward interpretation and calculations can be done with early and preliminary input  
73 data. For its part, ANN is used as the most accurate model, although the output calculation is  
74 not as "clear" as in the case of PR due to the difficulty of interpreting the structure of the  
75 resulting ANN. ANN are expected to be used with the final input data.

76 Three East Indian regions where agriculture plays an important role were chosen as a case  
77 study. ML models were built for the period 1967-2015. ML models aim to predict rice crop  
78 yield since rice is the most cultivated crop in these regions. The ML approach was applied  
79 separately to the three regions.

#### 80 **Crop yield prediction in India**

81 In India, as in many other countries, the official crop yield prediction is mainly based on  
82 conventional data collections techniques such as ground-field visits (Reynolds et al., 2000;  
83 Sawasawa, 2003). The crop yield is measured through crop cutting experiments carried out  
84 over sample crop areas. In this country, principal crops' calculations of area and yield are  
85 released through the Directorate of Economics and Statistics, Ministry of Agriculture  
86 (DESMOA). The production (in kg or ton) of a specific crop is calculated by multiplying the  
87 whole field area by its crop yield. The crop production is needed for the decision-makers to  
88 take various policy decisions relating to pricing, marketing, distribution, exportation and  
89 importation.

90 The Kharif season, as it is locally known, represents about 80% of the annual rainfall (Naresh  
91 Kumar et al., 2012). This monsoon season generally goes from June to October. In this season,  
92 the highest agricultural production is obtained. Estimation of Kharif crop yield and production  
93 is released four times during the year with different levels of sophistication and precision,  
94 where the last one is considered the most accurate. The first calculation is presented in  
95 September, the second one in January, the third one in March/April, and the fourth, and the last  
96 one in June/July. It should be noted that the last two calculations of crop yield and production  
97 become available much after the crops have already been harvested in December/January.  
98 From the four calculations, the first two can be considered as predictions. These two first  
99 predictions serve as primary estimations about how much the final yield and production will  
100 be.



101 The existing ground-field visits-based agricultural forecasting system provides reliable  
102 information; however, it lacks pre-harvesting forecasting. This limitation motivated the  
103 creation of a satellite-based forecasting system to have information at the early stages of crop  
104 growth. This system is called the National Crop Forecasting Centre (NCFC) (Sawasawa, 2003).  
105 NCFC is continuously verified and continuously updated. Although NCFC advances the one  
106 based on ground-field visits, data needed for its execution could be not always available.  
107 Therefore, it is necessary to explore other solutions. In this study, it is not intended to replace  
108 the previous and new forecasting systems, but to provide a complement to corroborate both  
109 estimates, and in a broader sense, to provide the scientific community with an approach to crop  
110 yield prediction with information on the spatial extent of drought.

## 111 **2 ML modelling methodology**

112 The experiment was carried out with the following methodology that involves the ML  
113 construction. The next paragraphs show each step in detail. These steps are (1) data preparation,  
114 (2) input variable selection, (3) polynomial regression models calculation, (4) artificial neural  
115 network models calculation, and (5) models application and combination.

### 116 **2.1 Step 1. Data preparation**

117 Two types of data were prepared, the crop yield and the percentage of drought areas. For data  
118 preparation, three tasks were carried out (1) data retrieving, (2) drought areas calculation, and  
119 (3) data de-trending.

#### 120 **2.1.1 Data retrieving**

121 Section 3 shows what corresponds to data retrieving for crop yield (CY) and the drought  
122 indicator. CY data correspond to the largest growing season. CY time series has a value for  
123 each year for the period 1966-2015 (49 years). CY was available for each region. On the other  
124 hand, drought indicator data is on a monthly basis for the period 1901-2015. The spatial  
125 resolution is half a degree.

#### 126 **2.1.2 Drought areas calculation**

127 The drought areas were calculated following the methodology presented below. These areas  
128 were calculated for the three regions. Drought areas were calculated from the drought indicator  
129 data that is in a grid format, i.e., each cell has associated a geographic location and a time step.  
130 The calculation of drought areas started with the reclassification of all the cells of the drought  
131 indicator data by non-drought and drought cells. The drought indicator data was evaluated cell  
132 by cell to determine those that are in drought, i.e. drought condition. To determine drought and  
133 non-drought condition ( $D_s$ ), the Eq. 1 was applied (Corzo Perez et al., 2011; Diaz et al., 2019,



134 2020; Herrera-Estrada et al., 2017). Eq. 1 represents the following. When the drought indicator  
135 is below to the selected threshold  $T$ , the value of 1 is used to indicate drought in the cell and  
136 non-drought is represented by the value of 0. This classification is performed for all the cells  
137 of the grid data in each time step ( $t$ ).

$$138 \quad D_s(t) = \begin{cases} 1 & \text{if } DI(t) \leq T \\ 0 & \text{if } DI(t) > T \end{cases} \quad (\text{Eq. 1})$$

139 Once the ones-and-zeros data was obtained, the drought areas (DAs) were calculated for each  
140 region with Eq. 2. DA was computed as the ratio between the cells in drought and the total  
141 number of cells of the region ( $N$ ). In Eq. 2, the number of cell is denoted by  $c$ .

$$142 \quad DA(t) = 100/N \cdot \sum_{c=1}^N D_s(t) \quad (\text{Eq. 2})$$

143 The number of cells ( $N$ ) of the mask is 63, 31 and 54 for region 1, 2 and 3. The masks in raster  
144 format were built for each region. The mask is an array of ones and zeros, where the value of  
145 1 indicates the land. We used the threshold  $T = -1$  to calculate cells in droughts. This threshold  
146 is widely used to identify a cell in drought when working with standardised indices such as the  
147 used in this research (Sect. 3.2). Usually, drought indicator data is calculated at different  
148 aggregations periods. We retrieved this data for 1, 3, 6, 9, and 12 months of aggregation period  
149 (Sect. 3.2). DAs' time series were calculated for each aggregation period and are indicated as  
150 DA1, DA3, DA6, DA9, and DA12.

### 151 2.1.3 Data de-trending

152 Data stationarity is typically assumed when modelling. However, the present study uses crop  
153 yield, which is non-stationary in nature. The crop yield depends on factors that affect its trend,  
154 such as drought, flood, cultivars and its own management. Therefore, it is advisable to remove  
155 short-term fluctuations in crop yield before constructing the model (Montesino Pouzols and  
156 Lendasse, 2010).

157 Among the methods available to de-trend data, the 'first difference' method is popular due to  
158 its simplicity. In this method, the trend is removed from the time series by subtracting the  
159 previous value  $x^*(t-1)$  from the current one  $x^*(t)$ , as shown in Eq. 3. The de-trended value for  
160 the first time step ( $t = 1$ ) is not calculated. The length of the de-trended time series is  $n = m - 1$ ,  
161 where  $m$  is the length of the original time series. The de-trended data  $x(t)$  has the same units as  
162 the original data  $x^*(t)$ .

$$163 \quad x(t) = x^*(t) - x^*(t-1) \quad (\text{Eq. 3})$$

164 The trended of CY and DA time series was removed with Eq. 3. For the case of CY, the de-  
165 trended time series retained one value per season, i.e. one per year. As noted, the method for



166 removing the trend does not generate the value for the first time step; therefore, the de-trended  
167 CY data corresponds to the period 1967-2015 (49 years).

168 In the case of DA, Eq. 3 was applied as follows. Because the DA data is monthly, i.e. 12 values  
169 per year, and CY data is seasonal, i.e. one value per year, first DA time series were extracted  
170 for each month. The monthly values for January were extracted for each year and so on until  
171 December. These twelve DA time series were compiled for each of the five DA1, 3, 6, 9 and  
172 12 time series. A total of 60 DA time series ( $12 \times 5$ ) were obtained. To refer to these time  
173 series, a number (suffix) was added to indicate the month. In this way, for example, the time  
174 series DA3\_7 indicates the drought areas for July calculated from the drought indicator with  
175 3-month aggregation period. Eq. 3 for the removal of the trend was applied to each of the 60  
176 DA time series. The DA time series run from 1901-2015. For the construction of the ML  
177 models, the common period 1967-2015 (49 years) was chosen.

## 178 **2.2 Step 2. Input variable selection**

179 In an ML model, the input, known as the predictor, is generally made up of independent  
180 variables. Often these variables are arranged in different ways to determine the best model  
181 input representation. An example arrangement is the selection of the independent variable using  
182 different previous time steps, such as  $t-1$  (the previous time),  $t-2$  and so on. When using  
183 drought indicators as the predictors, these arrangements include the different aggregation  
184 periods (i.e. different aggregation periods are tested). The idea is not to include all the variables  
185 and all their different possible arrangements but rather to find the best ones and discard those  
186 that do not contribute significantly to the model's results. Other arrangements of the input  
187 variable include the average, or other statistics, over a period.

188 There are different methods for selecting input variables. Based on the procedure, these  
189 methods are classified into model-based and filter types (May et al., 2011). The first includes  
190 all those where the model runs, and based on its performance, a specific variable is chosen or  
191 discarded. The latter include methods where the variable is chosen *a priori* through a generally  
192 statistical process and does not require the model to be run. Correlation analysis, which falls  
193 under the second category, is often chosen for its simplicity and wide application. Correlation  
194 is calculated between the time series of the output variable (CY in this case) and the different  
195 input variables, including their various arrangements.

196 In this study, for the selection of the relevant input variables, the correlation analysis was done.  
197 The correlation was calculated between the de-trended time series of the seasonal CY and the  
198 60 DAs. As mentioned before, due to DAs are monthly and CY is seasonal, 12 time series of



199 DAs were prepared, one per month, for each aggregation period. The DAs were then correlated  
200 with the CY. Another option could be to use the yearly average value of the DAs, such as the  
201 average of the DAs of the months of the cultivation period, or something similar. However, we  
202 opted to identify the DAs of the months that have the highest correlation with the seasonal CY  
203 and use them as inputs.

204 The approach of the selection of the most correlated DAs was chosen for two main reasons.  
205 On the one hand, rice responds to the climate variations differently from one growth stage to  
206 another over the year, which could be better captured with the information of some months  
207 than others. On the other hand, different types of drought (i.e. meteorological, agricultural, and  
208 hydrological) are expected to affect (impact) the crop yield to different degrees. This level of  
209 affectation could be taken into account either by using different hydro-meteorological variables  
210 or selecting different aggregation periods of the meteorological variables, as in this case. An  
211 average of DAs could "hide" a significant drought area that could contribute more (or less) to  
212 the final crop yield. In addition, in this research, ML models were built to be used at different  
213 stages of crop cultivation, i.e. models to be applied in June, July, and so on, each of them with  
214 a different expected degree of accuracy. Therefore, the use of time series for each month  
215 extracted from the DAs for all the different aggregation periods is more appropriate.

216 Based on the correlation coefficient, the input variables were selected. In total, 15 sets of input  
217 variables (Table 2) were selected for each month from January to December. Each set is made  
218 up of different DA time series, out of the 60 de-trended DAs. The number of variables is  
219 different in each set. These sets of input variables are presented in the results section. All sets  
220 include the de-trended CY from the previous year ( $CY_{t-1}$ ).  $CY_{t-1}$  was used because, in the  
221 particular case of the study area, CY of the current year is planned to be reached based on data  
222 of the previous year.

### 223 **2.3 Step 3. Polynomial regression models calculation**

224 For the case of PR, four types of models were tested (Table 1). All the PR models were built  
225 for each month from January to December following Eq. 5 to 8. A total of 15 sets of  
226 combinations of input variables were tested in each PR model. The best PR model was  
227 identified for each month following the RMSE criterion (Eq. 9). MATLAB software was used  
228 for implementation.

229 PR is an extension of linear regression that allows the use of more than one input variable to  
230 calculate the output variable (Eq. 4).



$$231 \quad y = b_0 + \sum_{i=1}^n b_i x_i + e \quad (\text{Eq. 4})$$

232 In Eq. 4,  $y$  is the output variable, also known as the response, which in this case is the crop  
 233 yield. The term  $x_i$  is the  $i$ -th input variable (predictor) from a total of  $n$  variables. The regression  
 234 coefficients vector is represented by  $b$ . From the coefficients vector,  $b_0$  is known as the  
 235 intercept. The vector of errors is indicated by  $e$ .

236 Table 1 shows four formulations of PR. The PR models are indicated as linear, pure-quadratic,  
 237 quadratic and interactions. Descriptions of each and their equations are presented in Table 1  
 238 (Eq. 5 to 8). The input variable ( $x_i$ ) was selected based on the correlation analysis (Sect. 2.2).

239 **Table 1** Polynomial regression (PR) types followed in this study.

PR type	Equation	Description
Linear	(Eq. 5) $y = b_0 + \sum_{i=1}^n b_i x_i$	It has an intercept and linear terms of predictors
Pure-quadratic	(Eq. 6) $y = b_0 + \sum_{i=1}^n b_i x_i + \sum_{i=1}^n b_{n+i} x_i^2$	It has an intercept, as well as linear and squared terms of predictors
Quadratic	(Eq. 7) $y = b_0 + \sum_{i=1}^n b_i x_i + \sum_{i=1}^n b_{n+i} x_i^2 + \sum_{i=1}^{n-1} \sum_{j=i+1}^n b_{2n+(i-1)n-\frac{(i-1)i}{2}+(j-i)} x_i x_j$	It has an intercept, linear and squared terms and all products of pairs of distinct predictors
Interactions	(Eq. 8) $y = b_0 + \sum_{i=1}^n b_i x_i + \sum_{i=1}^{n-1} \sum_{j=i+1}^n b_{n+(i-1)n-\frac{(i-1)i}{2}+(j-i)} x_i x_j$	It has an intercept, linear terms of predictors, all products of pairs of distinct predictors and no squared terms

240

241 The best PR model was identified from four types using the root mean square error (RMSE)  
 242 criterion. The RMSE is calculated between the observations ( $o$ ) and the predictions ( $p$ ), as  
 243 shown in Eq. 9. RMSE is one of the most widely used criteria in the comparison of observations  
 244 and model calculations.

$$245 \quad \text{RMSE} = \sqrt{\frac{\sum_{i=1}^n (o_i - p_i)^2}{n}} \quad (\text{Eq. 9})$$

#### 246 **2.4 Step 4. Artificial neural network models calculation**

247 ANN is a method loosely based on imitating the basic functionality of neurons (i.e. the working  
 248 units of the human brain) (Govindaraju, 2000; Maier and Dandy, 2000). The input variables





249 (predictors) are connected to each other through mathematical formulations that allow complex  
250 non-linear relationships to be represented. These connexions are symbolised as nodes  
251 interconnected within a network aimed at calculating the output variable (response).  
252 Of the different proposed ANN architectures (network designs), one of the most widely used  
253 is the feedforward neural network (FFNN). The FFNN is schematised by a series of nodes  
254 located in one of three layers: input, hidden or output. The number of input nodes is equal to  
255 the number of input variables in the input layer (Elshorbagy et al., 2010). This first layer is in  
256 turn connected to the hidden layer, which receives this name because the connections made  
257 there may not be immediately evident to the model performer. In this hidden layer, the number  
258 of nodes is not defined by default; rather, the greater the number of nodes, the more complex  
259 the model. Finally, the nodes of the hidden layer are connected to those of the output layer. In  
260 a single-output variable problem, there is only one node. ANNs are typically trained by non-  
261 linear optimisation gradient-based algorithms, e.g. the Levenberg-Marquardt algorithm.  
262 In the ANN setup, the number of nodes of the input layer was equal to the number of variables  
263 of the respective combination. The number of nodes in the output layer was one and  
264 corresponded to the seasonal crop production (CY). An iteration optimisation procedure was  
265 carried out regarding the hidden layer, varying the number of nodes from 1 to 10. For each  
266 number of nodes, 100 iterations were done, being 1,000 in total. For reproducibility of the  
267 results, the random values were set to default at the beginning of the number of nodes change.  
268 For each month, from January to December, the ANNs were built. MATLAB software was  
269 used to implement the ANNs with the Levenberg-Marquardt algorithm for training. In each of  
270 the ANNs, 85 % of the data was used for training-validation, and the rest for testing  
271 (verification). The best model corresponding to each number of hidden nodes was identified,  
272 i.e. ten models per month and the best model for each month. RMSE was used to identify the  
273 best models. RMSE was calculated for (1) the training-validation dataset (RMSE\_cal), (2) the  
274 testing dataset (RMSE\_test), and (3) the entire period (RMSE). In all the cases, the final (best)  
275 model was chosen based on RMSE for the entire period.

## 276 **2.5 Step 5. Models application and combination**

277 Once the best ML models, PR and ANN, were known, the pair of models were selected for  
278 each month. Depending on the performance of these models (and experience of their use), they  
279 can be used either separately or combined, e.g. being run in parallel so that a modeller could  
280 see the cases when models produce different results. An alternative is to use a dynamic



281 weighting of the models' outputs (e.g. with the weights being proportional to the historical  
282 performance) to form a "model committee".

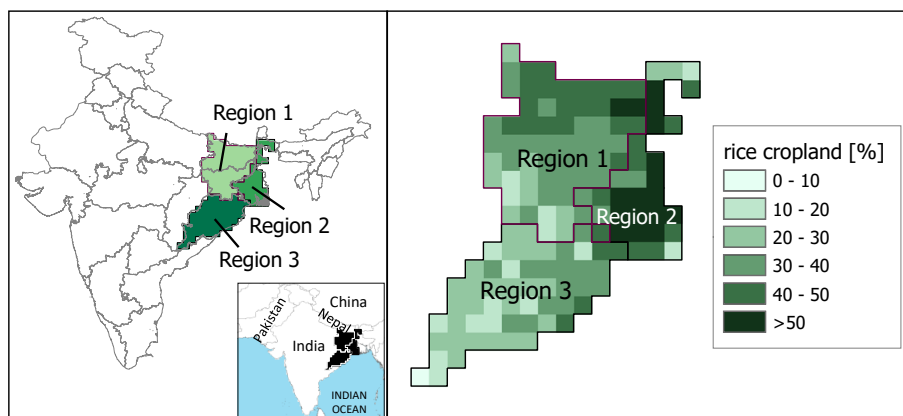
### 283 **3 Data**

#### 284 **3.1 Crop yield**

285 Rice is the most important food grain in East India, so it was selected to assess our ML-oriented  
286 crop-yield predictions. Rice from this region accounts for roughly 85 percent of the total rice  
287 production in India (Ghosh et al., 2014). As mentioned, ML models were constructed for three  
288 regions of the eastern Indian (Figure 1). State-wise crop-yield data was retrieved from 1966 to  
289 2015 (49 years) through the Indian Directorate of Economic and Statistics from the Department  
290 of Agriculture (DAC) (<http://eands.dacnet.nic.in/>).

291 There are three crop seasons in India: Rabi, Kharif and Zaid. Of these, the Kharif season was  
292 chosen for study because it is the largest in terms of crop production. Kharif crops are sown in  
293 June and harvested in November/December. Seasonal crop-yield data was obtained from the  
294 DAC website and arranged into time series per region. One value was assigned to each year of  
295 crops harvested in the Kharif season.

296 Figure 1 shows the location of the three regions. These are made up as follows. Region 1  
297 includes the current states of Bihar and Jharkhand; region 2 corresponds to the state of West  
298 Bengal; and region 3 makes up the state of Odisha. Two important clarifications have to be  
299 made regarding crop yield data retrieving for these regions. First, in late 2000, Bihar was  
300 divided into two states: Bihar and Jharkhand. Thereafter, rice data was reported separately. In  
301 this study, both states are marked as region 1; the crop-yield data from 2000 to 2015 is the  
302 reported sum of current Bihar and Jharkhand. Second, in 2011, Orissa was renamed Odisha  
303 (region 3), but the territory remains the same. In this case, crop yield data for Odisha is that  
304 reported for the former Orissa and the current Odisha.



305  
306 **Figure 1** Case study location and rice cropland (in percentage). Case study comprises region 1 (Bihar and  
307 Jharkhand), region 2 (West Bengal) and region 3 (Odisha). Source of rice cropland: Monfreda et al. (2008).

### 308 **3.2 Drought indicator**

309 Soil moisture is the preferred variable for calculating agricultural drought indicators. However,  
310 another widely disseminated way to indirectly infer this type of drought indicator is to use  
311 meteorological drought indicators as proxies. Among these, the Standardised Precipitation  
312 Evaporation Index (SPEI) proposed by Vicente-Serrano et al. (2010) has shown to be useful in  
313 assessing agricultural drought. The SPEI follows a similar methodology as that of the widely  
314 used Standardized Precipitation Index (SPI) (McKee et al., 1993), but with added consideration  
315 for the difference between precipitation and evapotranspiration. SPEI data was retrieved from  
316 the SPEI Global Drought Monitor (<https://spei.csic.es>) between 1901 and 2015. The spatial  
317 resolution of the drought indicator data is 0.5 degrees. The SPEI data was available at different  
318 aggregation periods; for this study, it was retrieved for the aggregation periods of 1, 3, 6, 9 and  
319 12 months, indicated as DI1, DI3, DI6, DI9 and DI12, respectively.

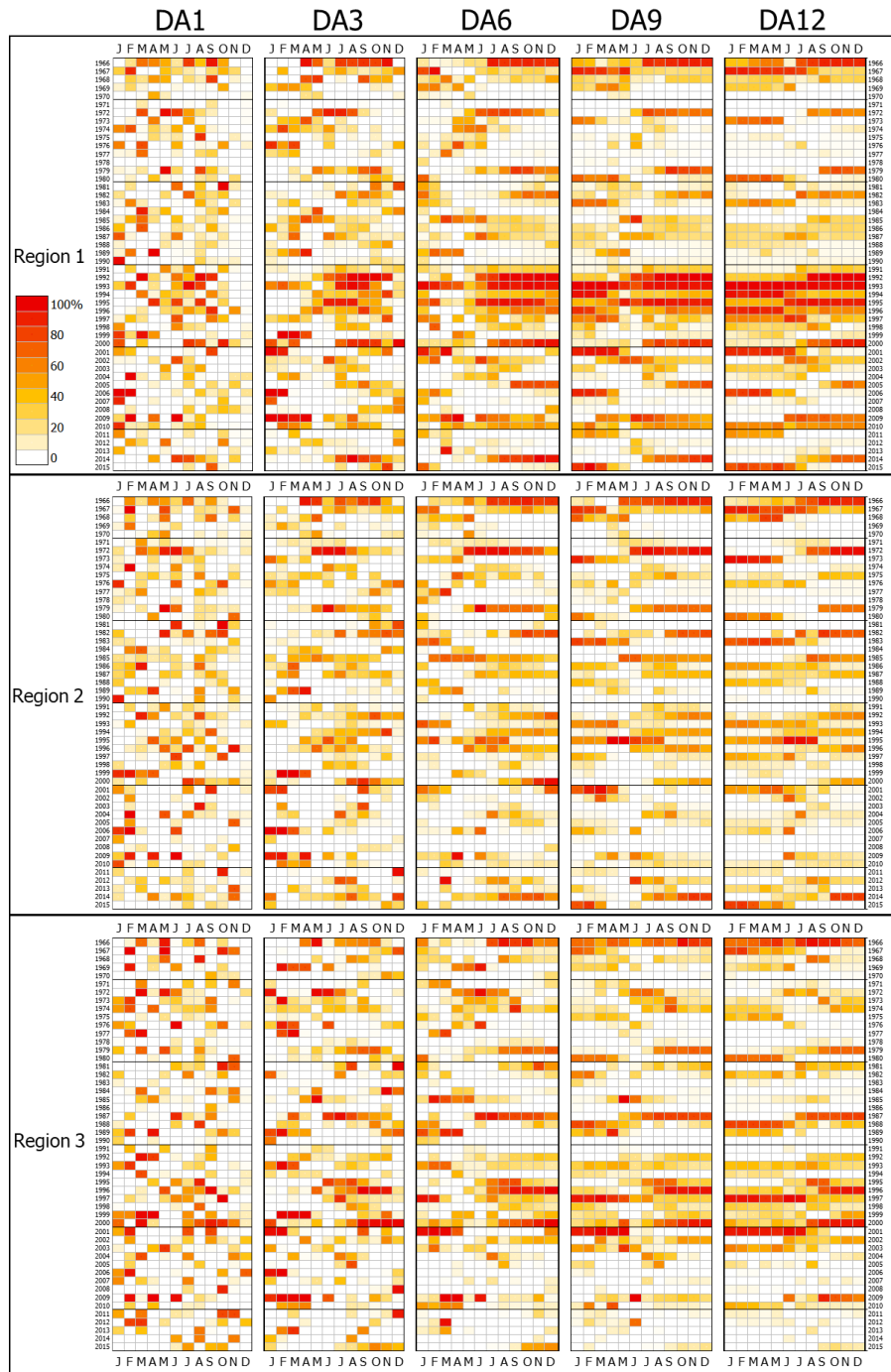
## 320 **4 Results and discussion**

### 321 **4.1 Data preparation: drought areas and crop yield**

322 Figure 2 show the drought areas calculated for the three regions. In this heat map, columns  
323 indicate the months and rows point out the years. The redder the colour, the larger the drought  
324 area. In general, region 1 (Figure 2, the upper panel) presents the highest values concerning the  
325 other two regions. In general, the 1990s show higher values of areas with respect to the rest of  
326 the period, which agrees with Guha-Sapir (2019); in this decade, there were three droughts,  
327 1993, 1996 and 2000. At the beginning of the period, large areas are also observed in the three  
328 regions; these results align with Bhalme and Mooley (1980).



329 In Figure 2, a pattern is observed in the drought areas distribution for all the aggregation  
330 periods, i.e. from DA1 to DA12. In DA1, the areas mainly concentrate in the first months; even  
331 the December column is almost white (without drought). Later, for DA3, the large areas are  
332 located from April to November. Successively, for DA6 and DA9, the largest areas are  
333 concentrated in the second half of the year. There are even droughts that end in the following  
334 year; they are the reddish lines that are observed in the first semester (first columns). Finally,  
335 in DA12, there are consecutive large areas indicated by the reddish lines; droughts usually  
336 begin in the second semester and extend until the following year. These results show the  
337 importance of considering more than one period of aggregation when using indicators based  
338 on meteorological variables; each aggregation period can be a proxy for analysing different  
339 types of drought and its effects.



340  
 341 **Figure 2** Drought areas (DAs) for each aggregation period (1, 3, 6, 9 and 12 months) and region. Top, middle,  
 342 and bottom panels indicate region 1 (Bihar and Jharkhand), region 2 (West Bengal) and region 3 (Odisha).



343 Figure 3 shows the time series of de-trended CY and DA for the three regions. In the case of  
344 DA (indicated in red), the values are displayed in inverse order to facilitate interpretation. In  
345 general, when drought areas increase, this is expected to affect crop yield (decreasing).  
346 Otherwise, when the drought area decreases, this effect favours an increase in crop yield. In  
347 general, for the three regions, the decreases in CY coincide with the increases in DA. The  
348 general pattern regarding DA variations is as follows. The values fluctuate throughout the year  
349 for the aggregation periods of one and three months (DA1 and DA3). Subsequently, for DA6  
350 to DA12, the values are concentrated in the second half of the year. These results also show  
351 the usefulness of the different aggregation periods to capture different types of drought. The  
352 effect of increasing DA seems not to be observed in decreasing CY for all cases of DAs. For  
353 example, in region 1 (Figure 3, the upper panel), the decrease in 2004, one of the maximums,  
354 does not coincide with increases in DA9 and DA12, but it does for DA1, DA3 and DA6. These  
355 results also support the use of the different aggregation periods on drought assessments.

#### 356 **4.2 Input variable selection (correlation analysis)**

357 Figure 4 summarises the correlation between the de-trended CY and the DAs, and Figure 5  
358 presents the correlation for each monthly DA time series.

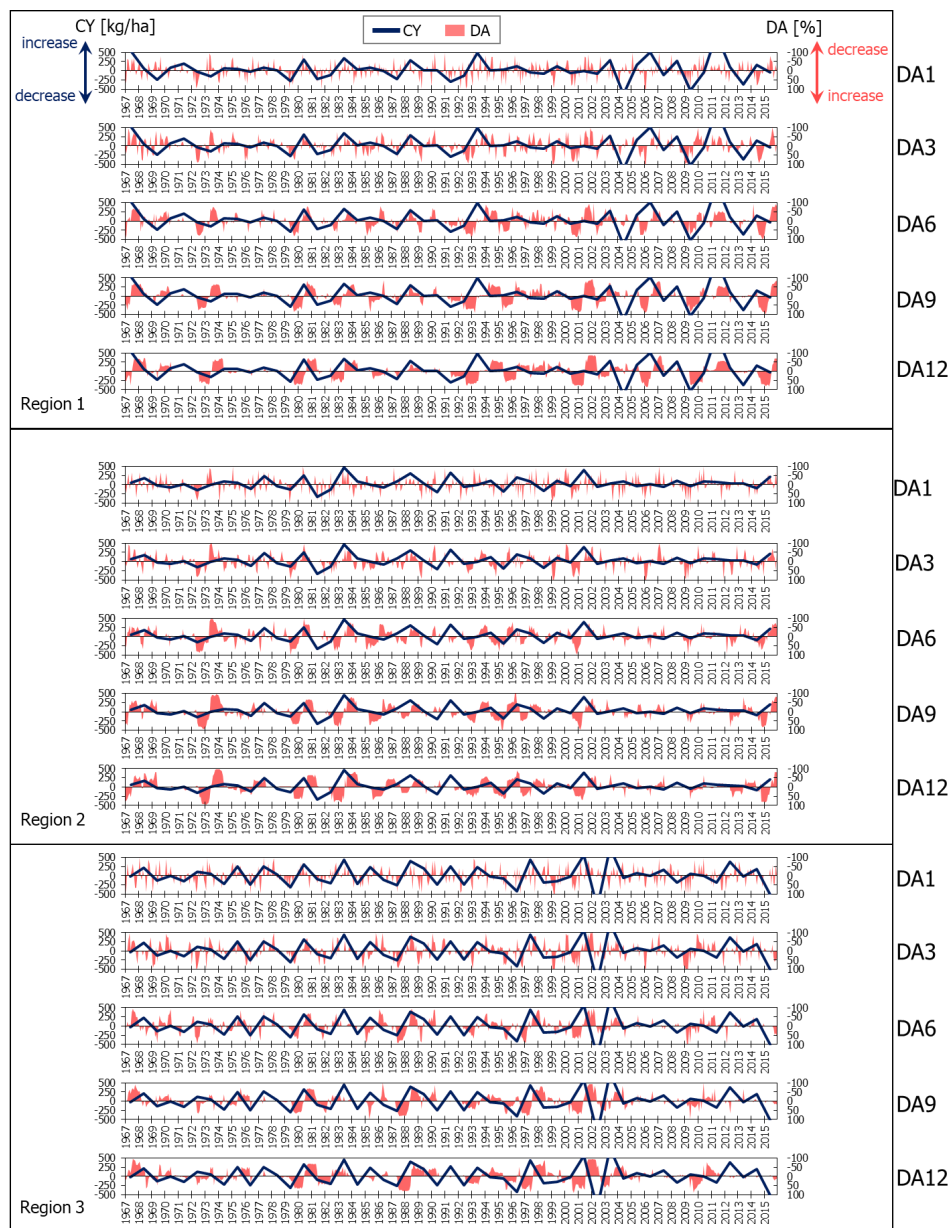
359 Figure 4 and 5 shows that the correlation is different over the year in the three regions. In all  
360 cases, the correlation coefficient increases until a maximum and then decreases. The month in  
361 which the maximum value is reached is different for each region but falls within the crop season  
362 (i.e. June to November/December). For region 1, it is in July. For region 2, there are four  
363 months with this pattern, June, July, October, and November. Finally, for region 3, it is  
364 October, November and December.

365 These results of correlation can be useful for monitoring agricultural drought. For example, in  
366 region 1, the drought areas calculated from SPEI6 (i.e. DA6) show a maximum correlation in  
367 July. This correlation value means that the previous six months' accumulated effect is crucial  
368 for the crop yield of the Kharif season, which covers more or less from June to  
369 November/December.

370 Figure 4 shows the following pattern. In general, for region 1, results similar to DA6 are  
371 observed for DA3, 9 and 12. For region 2, a similar pattern happens in the peaks, but in this  
372 case two, one corresponding to DA1 and 3, and the other to DA6, 9, and 12. The first peak of  
373 DA1 and DA3 may indicate that it is crucial to pay attention to the immediate period conditions  
374 of one to three months. In the case of the second peak, the medium and long-term conditions,  
375 6 to 12 months, are more important to monitor for the harvest month. For region 3, the peak



376 occurs at the end of the growing season, in almost all cases. Hence, the condition before the  
 377 growing season is decisive for the crop yield.  
 378

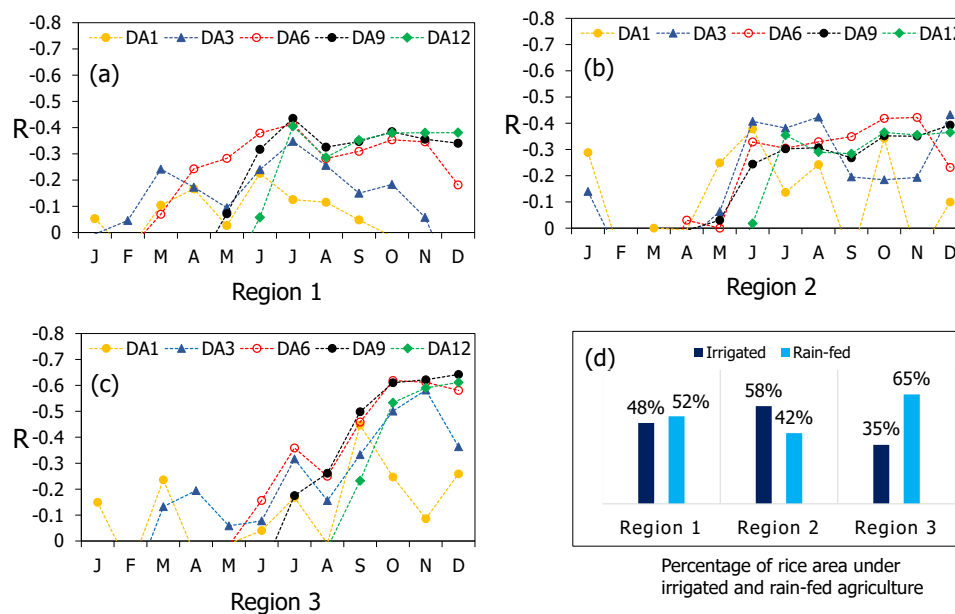


379  
 380 **Figure 3** Time series of the de-trended crop yield (CY) and drought areas (DAs) for each aggregation period (1,  
 381 3, 6, 9 and 12 months) and region. Top, middle, and bottom panels indicate region 1 (Bihar and Jharkhand), region  
 382 2 (West Bengal) and region 3 (Odisha).



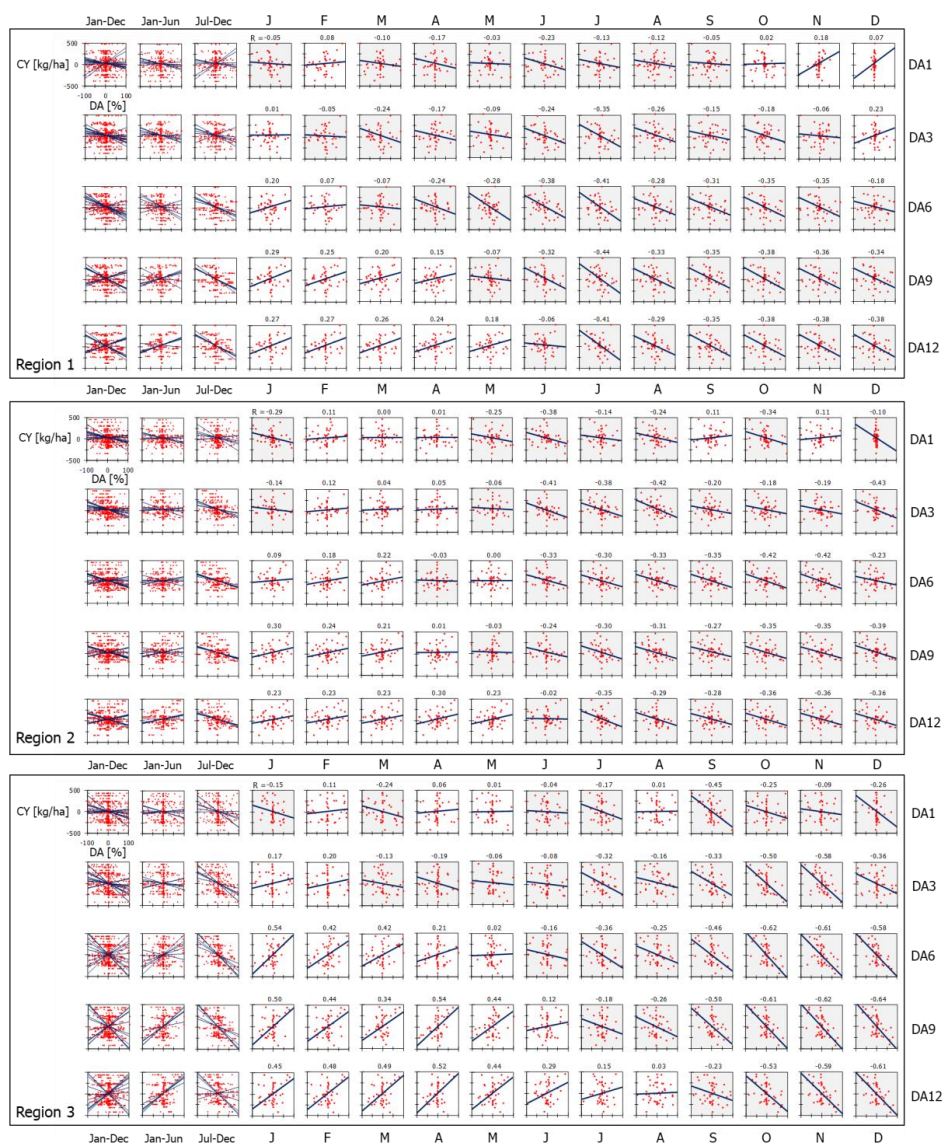
383 Figure 5 shows how the correlation coefficients between CY and DA are positive outside the  
 384 growing season and negative within that season. However, this pattern is less evident for DA1  
 385 and DA3. The pattern shown by the correlation coefficients in Figure 5 supports the idea that  
 386 drought is an important factor in crop yield since the months with less drought are more  
 387 correlated with the increase in CY, and the months with more drought do so with decrease in  
 388 CY.

389 Figure 4 (d) shows the percentage of irrigated and rain-fed agriculture. For regions 1 and 2,  
 390 about half is by irrigation, while in region 3, only 35%. Perhaps this percentage of irrigation  
 391 for region 3 explains why the correlation coefficients for this region are higher than for the  
 392 other two (Figure 4, and 5 (c)). Region 3 is more dependent on rain for agriculture; therefore,  
 393 this condition is best captured when calculating drought with the precipitation, as in this case  
 394 (Sect. 3.2).



395  
 396 **Figure 4** Summary of correlation between de-trended crop yield (CY) and drought areas (DAs) for each  
 397 aggregation period (1, 3, 6, 9 and 12 months) and region: (a) region 1 (Bihar and Jharkhand), (b) region 2 (West  
 398 Bengal) and (c) region 3 (Odisha). Percentage of rice area under irrigated and rein-fed agriculture (d). Source of  
 399 irrigated and rein-fed agriculture data: Directorate of Rice Development (DRD), (2014).





400  
 401  
 402  
 403  
 404  
 405  
 406  
 407

**Figure 5** Correlation between de-trended crop yield (CY) and drought areas (DAs) for each aggregation period (1, 3, 6, 9 and 12 months) and region. Results are shown for each monthly DA time series from June to December (J to D). Top, middle, and bottom panels indicate region 1 (Bihar and Jharkhand), region 2 (West Bengal) and region 3 (Odisha).



408 Figure 4 (a, b, and c) shows the following pattern in the three regions. The correlation  
 409 coefficients between CY and DAs increase according to the aggregation periods and the month  
 410 of analysis. DA1 and DA3 have a better correlation in the first months of the year. DA6 has a  
 411 better correlation in the subsequent months, between May and June. Finally, DA9 and 12 do  
 412 so within the second half of the year.

413 Each respective DA time series reaches a maximum (or maximums) of correlation, and then  
 414 correlation decreases. According to this pattern, the 15 combinations of input variables shown  
 415 in Table 2 were selected. As earlier mentioned, the CY of the previous year was included in all  
 416 combinations and is indicated as  $CY_{t-1}$ . Combinations 1 to 5 only include a DA time series.  
 417 Combinations 6 to 9 are DA pairs that were calculated with the drought indicator of successive  
 418 aggregation times. For example, combination 6 forms DA1 and 3, combination 7 includes DA3  
 419 and 6, and so on. Similarly, combinations 10 to 13 are proposed, but for triples. Combinations  
 420 13 and 14 are fourfold. Finally, the last combination (15th) is made up of all the DA series.

421 As mentioned, the models were built for each DA time series using the 15 combinations  
 422 corresponding to each month. For example, the monthly series of DAs extracted for January  
 423 were used for the case of January. These DAs are DA1\_1, DA3\_1, DA6\_1, DA9\_1 and  
 424 DA12\_1. The suffix indicates the month. Then, the different DA1\_1 to DA12\_1 were used  
 425 following the 15 combinations shown in Table 2 to build the ML models (ANN and PR) for  
 426 January. Similarly, it was carried out from February to December.

427 **Table 2** Input sets (combinations) to build the ML models. CY and DA stand for crop yield and drought area.  
 428 DAs are calculated with the drought indicator for the aggregate period of 1, 3, 6, 9 and 12 months.

Input set (combination)	Input variables
1	$CY_{t-1}$ , DA1
2	$CY_{t-1}$ , DA3
3	$CY_{t-1}$ , DA6
4	$CY_{t-1}$ , DA9
5	$CY_{t-1}$ , DA12
6	$CY_{t-1}$ , DA1,3
7	$CY_{t-1}$ , DA3,6
8	$CY_{t-1}$ , DA6,9
9	$CY_{t-1}$ , DA9,12
10	$CY_{t-1}$ , DA1,3,6
11	$CY_{t-1}$ , DA3,6,9
12	$CY_{t-1}$ , DA6,9,12
13	$CY_{t-1}$ , DA1,3,6,9
14	$CY_{t-1}$ , DA3,6,9,12
15	$CY_{t-1}$ , DA1,3,6,9,12

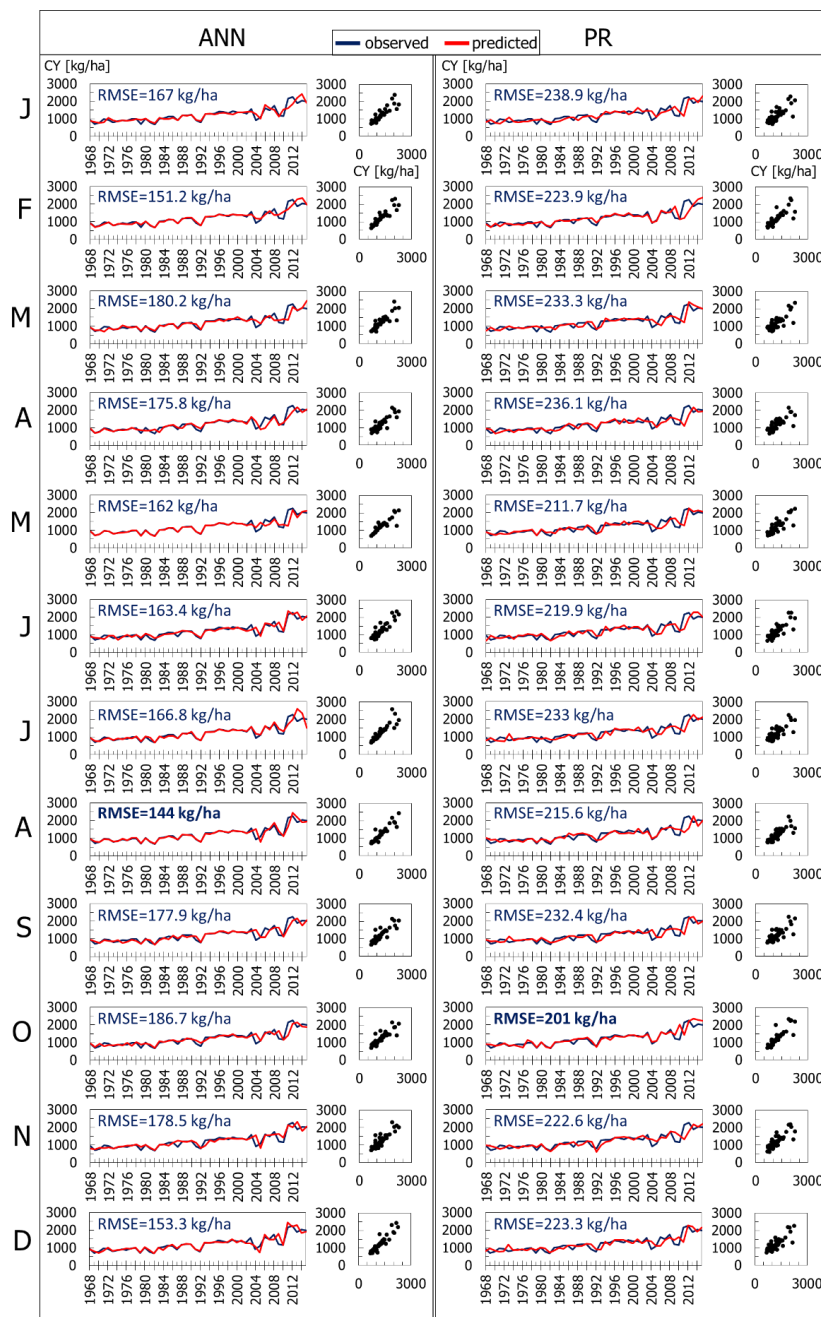


429 **4.3 ANN and PR models**

430 The results show different magnitudes of error between the observed and predicted CY. The  
431 models with the lowest error are presented in Figures 6, 7 and 8, for each of the three regions.  
432 The pair of ANN and PR that best predicts CY is shown for each month. The RMSE is also  
433 indicated in each case. On the other hand, Figure 9 shows the error for each input set  
434 (combination); the lowest error achieved in each month is presented in each case both for each  
435 ANN and PR.

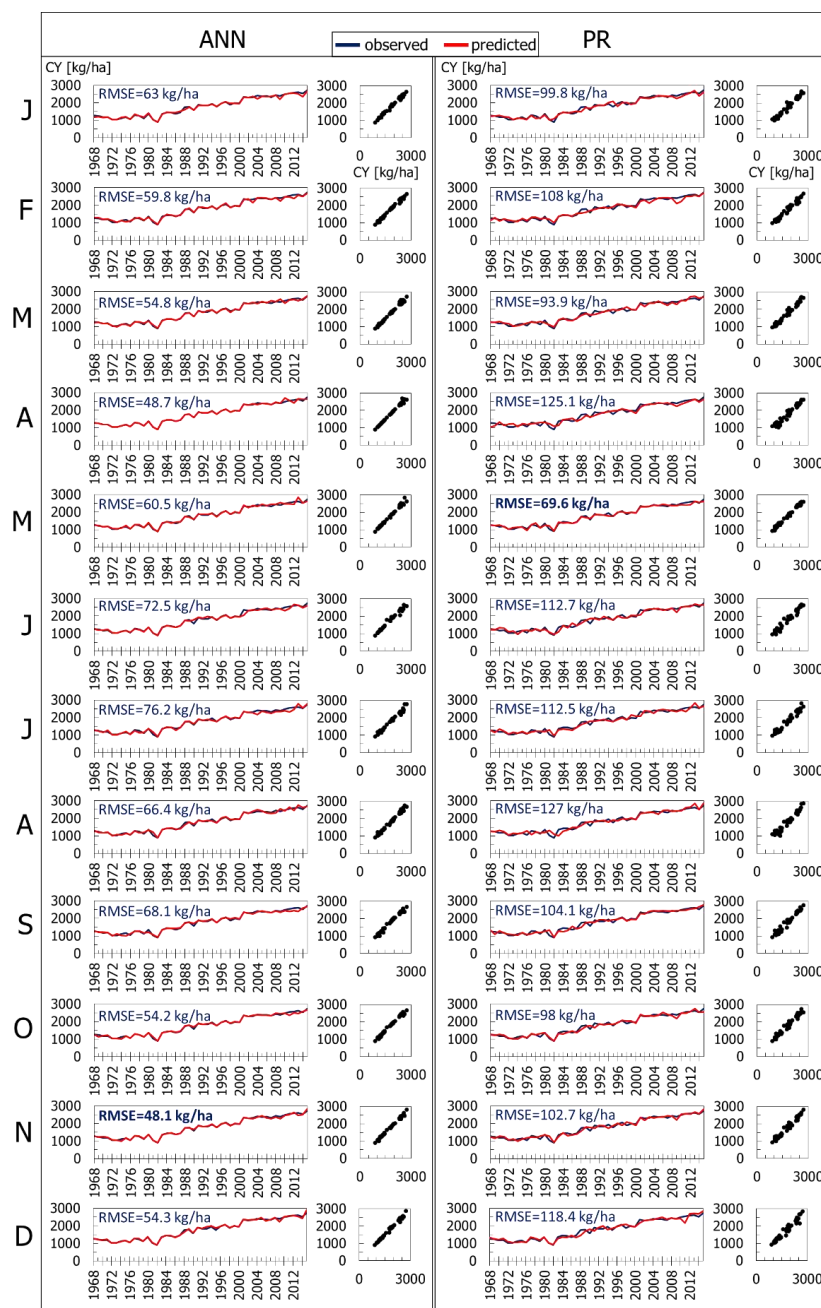
436 In general, ANN shows the least errors, as expected (Figure 9). However, the results of PR are  
437 not much worse compared to those of ANN; for example, in some cases, the errors shown by  
438 linear PR are very close to those of ANN (e.g. Figure 9, region 2). In general, it is observed  
439 that the models with the lowest errors correspond to region 2, followed by region 3 and region  
440 1 (Figure 9). It is attributed to the different degrees of crop irrigation with surface and mostly  
441 groundwater, which determines the accuracy of the modelling in the different regions. Another  
442 factor contributing to the models' performance is the drastic changes in the CY data, where  
443 regions 1 and 3 are the ones that presented the most, and to a much lesser extent, region 2.

444 Figure 9 shows that in the three regions, different types of PR showed better results. In general,  
445 linear and pure-quadratic indicate more stable results (no sudden changes among the different  
446 realisations) but not better than quadratic and interactions. In general quadratic and interactions  
447 present better results, being in some cases very close to those shown by ANN, e.g. PR  
448 interactions (Figure 9, region 1).



449

450 **Figure 6** ANN and PR models for predicting seasonal crop yield (CY) built for each time series of monthly  
 451 drought areas (DAs): region 1 (Bihar and Jharkhand). The model with the lowest error (RMSE) is presented for  
 452 each month, from January to December (J to D).



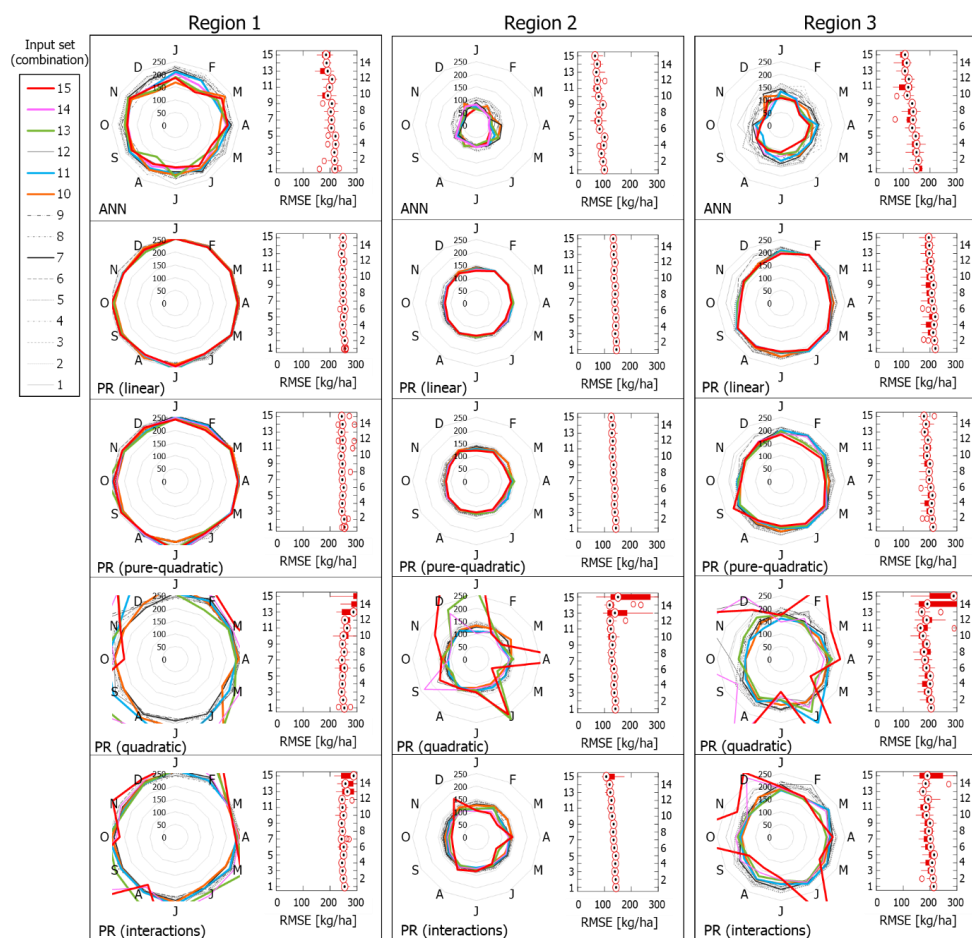
453

454 **Figure 7** ANN and PR models for predicting seasonal crop yield (CY) built for each time series of monthly  
 455 drought areas (DAs): region 2 (West Bengal). The model with the lowest error (RMSE) is presented for each  
 456 month, from January to December (J to D).





457  
 458 **Figure 8** ANN and PR models for predicting seasonal crop yield (CY) built for each time series of monthly  
 459 drought areas (DAs): region 3 (Odisha). The model with the lowest error (RMSE) is presented for each month,  
 460 from January to December (J to D).



461  
 462 **Figure 9** Root mean square error (RMSE) [kg/ha] for each of the 15 input sets (combinations) of the ANN and  
 463 PR models built for each region. For each set of input (from one to 15), the lowest errors are presented for each  
 464 month (January to December). Results of each input set are shown with lines to facilitate the analysis. Left, middle,  
 465 and right panels indicate region 1 (Bihar and Jharkhand), region 2 (West Bengal) and region 3 (Odisha).  
 466

#### 467 4.4 Models application and combination

468 The best performing models were selected for each month. Table 3 shows the summary of these  
 469 models, which includes the input set (combination), number of nodes, and errors for ANN, and  
 470 input set, type and errors for PR. The number of nodes indicates the degree of non-linearity  
 471 presented in each model. In this way, the more nodes, the more complex the model is in the  
 472 case of ANN. On the other hand, quadratic and interactions are the types that showed the best  
 473 performance in PR models. In all cases, within the combinations of input variables, a single  
 474 DA time series corresponding to one of the various aggregation periods (D1, D3, D6, D9 or



475 D12) that by itself produced good results was not found. The input sets are made up of two and  
 476 up to six different DAs corresponding to the various aggregation periods. Thus, using more  
 477 than one aggregation period of drought indicator results in better model performance.  
 478 Tables 4, 5 and 6 are derived from Table 3. These three tables show the PR formulas for region  
 479 1, 2 and 3, respectively. In each table, the PR formula and the inputs are indicated. These  
 480 formulas are also intended to be a stand-alone tool in the CY prediction for each region.  
 481 The proposed procedure for applying the ML models is as follows.  
 482 The calculation begins by selecting the formula of the PR model for each month. Then the CY  
 483 is calculated with the chosen formula and the corresponding input variables. At the same time,  
 484 or when it can be computed, the ANN model of the month under analysis is applied. An  
 485 alternative is to use an approach based on the dynamic weighting of the models' outputs to form  
 486 a model committee.

487 **Table 3** Summary of the ANN and PR models for predicting crop yield (CY) built for each month and region: (1)  
 488 Bihar and Jharkhand, (2) West Bengal and (3) Odisha. The table shows the models built with the lowest error  
 489 (RMSE). DA stands for drought area.

Region	ANN				PR			
	Month	Input set (combination)	No. nodes	RMSE [kg/ha]	Month	Input set (combination)	Type	RMSE [kg/ha]
Region 1	Jan	10 CY <sub>t-1</sub> , DA1,3,6	4	167.0	Jan	8 CY <sub>t-1</sub> , DA6,9	quadratic	238.9
	Feb	15 CY <sub>t-1</sub> , DA1,3,6,9,12	6	151.2	Feb	13 CY <sub>t-1</sub> , DA1,3,6,9	quadratic	223.9
	Mar	11 CY <sub>t-1</sub> , DA3,6,9	7	180.2	Mar	6 CY <sub>t-1</sub> , DA1,3	quadratic	233.3
	Apr	10 CY <sub>t-1</sub> , DA1,3,6	9	175.8	Apr	15 CY <sub>t-1</sub> , DA1,3,6,9,12	interactions	236.1
	May	15 CY <sub>t-1</sub> , DA1,3,6,9,12	5	162.0	May	10 CY <sub>t-1</sub> , DA1,3,6	quadratic	211.7
	Jun	13 CY <sub>t-1</sub> , DA1,3,6,9	2	163.4	Jun	10 CY <sub>t-1</sub> , DA1,3,6	interactions	219.9
	Jul	15 CY <sub>t-1</sub> , DA1,3,6,9,12	10	166.8	Jul	6 CY <sub>t-1</sub> , DA1,3	quadratic	233.0
	Aug	13 CY <sub>t-1</sub> , DA1,3,6,9	5	144.0	Aug	15 CY <sub>t-1</sub> , DA1,3,6,9,12	interactions	215.6
	Sep	6 CY <sub>t-1</sub> , DA1,3	5	177.9	Sep	7 CY <sub>t-1</sub> , DA3,6	quadratic	232.4
	Oct	14 CY <sub>t-1</sub> , DA3,6,9,12	6	186.7	Oct	15 CY <sub>t-1</sub> , DA1,3,6,9,12	quadratic	201.0
	Nov	8 CY <sub>t-1</sub> , DA6,9	4	178.5	Nov	13 CY <sub>t-1</sub> , DA1,3,6,9	interactions	222.6
	Dec	10 CY <sub>t-1</sub> , DA1,3,6	4	153.3	Dec	13 CY <sub>t-1</sub> , DA1,3,6,9	pure-quadratic	223.3
Region 2	Jan	13 CY <sub>t-1</sub> , DA1,3,6,9	8	63.0	Jan	14 CY <sub>t-1</sub> , DA3,6,9,12	quadratic	99.8
	Feb	11 CY <sub>t-1</sub> , DA3,6,9	10	59.8	Feb	15 CY <sub>t-1</sub> , DA1,3,6,9,12	interactions	108.0
	Mar	7 CY <sub>t-1</sub> , DA3,6	8	54.8	Mar	15 CY <sub>t-1</sub> , DA1,3,6,9,12	interactions	93.9
	Apr	14 CY <sub>t-1</sub> , DA3,6,9,12	7	48.7	Apr	14 CY <sub>t-1</sub> , DA3,6,9,12	interactions	125.1
	May	15 CY <sub>t-1</sub> , DA1,3,6,9,12	10	60.5	May	15 CY <sub>t-1</sub> , DA1,3,6,9,12	quadratic	69.6
	Jun	13 CY <sub>t-1</sub> , DA1,3,6,9	7	72.5	Jun	10 CY <sub>t-1</sub> , DA1,3,6	quadratic	112.7
	Jul	6 CY <sub>t-1</sub> , DA1,3	6	76.2	Jul	10 CY <sub>t-1</sub> , DA1,3,6	quadratic	112.5
	Aug	6 CY <sub>t-1</sub> , DA1,3	9	66.4	Aug	13 CY <sub>t-1</sub> , DA1,3,6,9	interactions	127.0
	Sep	6 CY <sub>t-1</sub> , DA1,3	10	68.1	Sep	15 CY <sub>t-1</sub> , DA1,3,6,9,12	interactions	104.1
	Oct	7 CY <sub>t-1</sub> , DA3,6	10	54.2	Oct	15 CY <sub>t-1</sub> , DA1,3,6,9,12	interactions	98.0
	Nov	7 CY <sub>t-1</sub> , DA3,6	10	48.1	Nov	15 CY <sub>t-1</sub> , DA1,3,6,9,12	interactions	102.7
	Dec	15 CY <sub>t-1</sub> , DA1,3,6,9,12	8	54.3	Dec	14 CY <sub>t-1</sub> , DA3,6,9,12	interactions	118.4
Region 3	Jan	15 CY <sub>t-1</sub> , DA1,3,6,9,12	7	106.5	Jan	14 CY <sub>t-1</sub> , DA3,6,9,12	quadratic	145.7
	Feb	13 CY <sub>t-1</sub> , DA1,3,6,9	10	105.7	Feb	10 CY <sub>t-1</sub> , DA1,3,6	quadratic	160.5
	Mar	15 CY <sub>t-1</sub> , DA1,3,6,9,12	9	84.1	Mar	12 CY <sub>t-1</sub> , DA6,9,12	quadratic	143.5
	Apr	15 CY <sub>t-1</sub> , DA1,3,6,9,12	4	112.3	Apr	14 CY <sub>t-1</sub> , DA3,6,9,12	quadratic	169.6
	May	12 CY <sub>t-1</sub> , DA6,9,12	10	100.3	May	15 CY <sub>t-1</sub> , DA1,3,6,9,12	quadratic	133.4
	Jun	15 CY <sub>t-1</sub> , DA1,3,6,9,12	9	94.5	Jun	12 CY <sub>t-1</sub> , DA6,9,12	quadratic	189.4
	Jul	15 CY <sub>t-1</sub> , DA1,3,6,9,12	7	106.0	Jul	15 CY <sub>t-1</sub> , DA1,3,6,9,12	quadratic	128.2
	Aug	12 CY <sub>t-1</sub> , DA6,9,12	7	103.9	Aug	15 CY <sub>t-1</sub> , DA1,3,6,9,12	interactions	137.7
	Sep	11 CY <sub>t-1</sub> , DA3,6,9	9	84.1	Sep	13 CY <sub>t-1</sub> , DA1,3,6,9	quadratic	145.0
	Oct	15 CY <sub>t-1</sub> , DA1,3,6,9,12	10	79.7	Oct	10 CY <sub>t-1</sub> , DA1,3,6	quadratic	139.0
	Nov	11 CY <sub>t-1</sub> , DA3,6,9	10	62.6	Nov	10 CY <sub>t-1</sub> , DA1,3,6	quadratic	127.5
	Dec	11 CY <sub>t-1</sub> , DA3,6,9	9	74.7	Dec	8 CY <sub>t-1</sub> , DA6,9	quadratic	137.3





491 **Table 4** PR models for predicting crop yield (CY) built for each month: region 1 (Bihar and Jharkhand). For each  
 492 moth, it is indicated the input (x1 to x6) and the PR formula. DA stands for drought area.

Month	Input						PR model
	x <sub>1</sub>	x <sub>2</sub>	x <sub>3</sub>	x <sub>4</sub>	x <sub>5</sub>	x <sub>6</sub>	
Jan	CY <sub>t-1</sub>	DA6	DA9				$-60.7111 - 0.1944x_1 - 0.2201x_2 + 1.2033x_3 - 0.0023x_1x_2 + 0.0043x_1x_3 - 0.0372x_2x_3 + 0.0003x_1^2 + 0.0504x_2^2 + 0.0308x_3^2$
Feb	CY <sub>t-1</sub>	DA1	DA3	DA6	DA9		$-27.4716 - 0.4688x_1 + 1.8718x_2 - 1.3313x_3 - 0.2611x_4 + 1.3878x_5 - 0.0137x_1x_2 + 0.0135x_1x_3 + 0.0032x_1x_4 + 0.0064x_1x_5 + 0.0823x_2x_3 + 0.0574x_2x_4 + 0.0935x_2x_5 - 0.0544x_3x_4 - 0.0746x_3x_5 - 0.0241x_4x_5 + 0.0014x_1^2 - 0.0496x_2^2 - 0.0202x_3^2 - 0.0016x_4^2 + 0.0227x_5^2$
Mar	CY <sub>t-1</sub>	DA1	DA3				$28.1213 - 0.5204x_1 - 0.4908x_2 + 0.0545x_3 + 0.0051x_1x_2 - 0.0093x_1x_3 + 0.0033x_2x_3 + 0.0003x_1^2 - 0.0107x_2^2 + 0.0086x_3^2$
Apr	CY <sub>t-1</sub>	DA1	DA3	DA6	DA9	DA12	$-24.3419 - 0.4785x_1 - 0.1965x_2 - 0.1356x_3 + 0.0848x_4 - 0.4774x_5 + 0.8029x_6 + 0.0066x_1x_2 + 0.0031x_1x_3 - 0.0128x_1x_4 + 0.0081x_1x_5 - 0.0003x_1x_6 + 0.0067x_2x_3 - 0.0604x_2x_4 + 0.1495x_2x_5 - 0.0169x_2x_6 + 0.0248x_3x_4 - 0.1295x_3x_5 - 0.0306x_3x_6 + 0.0458x_4x_5 + 0.0516x_4x_6 + 0.0595x_5x_6$
May	CY <sub>t-1</sub>	DA1	DA3	DA6			$113.2521 - 0.5132x_1 + 1.0101x_2 - 1.4019x_3 - 1.1130x_4 + 0.0100x_1x_2 + 0.0150x_1x_3 - 0.0027x_1x_4 + 0.0250x_2x_3 - 0.0655x_2x_4 + 0.0596x_3x_4 - 0.0006x_1^2 - 0.0358x_2^2 - 0.0380x_3^2 - 0.0495x_4^2$
Jun	CY <sub>t-1</sub>	DA1	DA3	DA6			$54.3 - 0.3715x_1 + 1.4832x_2 + 0.1432x_3 - 3.0648x_4 - 0.0106x_1x_2 + 0.0256x_1x_3 - 0.0111x_1x_4 - 0.0556x_2x_3 + 0.0648x_2x_4 - 0.0172x_3x_4$
Jul	CY <sub>t-1</sub>	DA1	DA3				$18.7237 - 0.3166x_1 + 1.3310x_2 - 3.0099x_3 - 0.0030x_1x_2 + 0.0024x_1x_3 + 0.0054x_2x_3 + 0.0001x_1^2 + 0.0065x_2^2 - 0.0065x_3^2$
Aug	CY <sub>t-1</sub>	DA1	DA3	DA6	DA9	DA12	$59.2373 - 0.6972x_1 + 0.1791x_2 + 5.1900x_3 - 1.3783x_4 - 6.9753x_5 + 1.5471x_6 - 0.0142x_1x_2 + 0.0072x_1x_3 + 0.1163x_1x_4 - 0.1285x_1x_5 + 0.0294x_1x_6 - 0.3670x_2x_3 + 0.0897x_2x_4 + 0.2332x_2x_5 + 0.0922x_2x_6 + 0.3014x_3x_4 + 0.3444x_3x_5 - 0.4160x_3x_6 - 0.5819x_4x_5 - 0.0450x_4x_6 + 0.3299x_5x_6$
Sep	CY <sub>t-1</sub>	DA3	DA6				$44.8563 - 0.4565x_1 + 0.6884x_2 - 1.9466x_3 + 0.0053x_1x_2 - 0.0005x_1x_3 + 0.0012x_2x_3 + 0.0004x_1^2 - 0.0172x_2^2 - 0.0002x_3^2$
Oct	CY <sub>t-1</sub>	DA1	DA3	DA6	DA9	DA12	$76.1546 + 0.0046x_1 - 2.2220x_2 + 1.0816x_3 + 19.1690x_4 - 53.2338x_5 + 29.1398x_6 + 0.0048x_1x_2 + 0.0155x_1x_3 - 0.0383x_1x_4 - 0.0868x_1x_5 + 0.1254x_1x_6 - 0.0444x_2x_3 + 0.0448x_2x_4 + 0.0175x_2x_5 - 0.0552x_2x_6 + 0.2154x_3x_4 - 1.0260x_3x_5 + 0.7776x_3x_6 + 3.2060x_4x_5 - 3.3267x_4x_6 + 11.6655x_5x_6 + 0.0002x_1^2 - 0.0547x_2^2 + 0.1171x_3^2 + 0.2874x_4^2 - 7.7995x_5^2 - 4.0845x_6^2$
Nov	CY <sub>t-1</sub>	DA1	DA3	DA6	DA9		$30.0286 - 0.4536x_1 - 0.6721x_2 - 0.8270x_3 - 7.0981x_4 + 5.3007x_5 - 0.0339x_1x_2 + 0.0086x_1x_3 + 0.0107x_1x_4 - 0.0084x_1x_5 + 0.1347x_2x_3 + 0.1123x_2x_4 - 0.0596x_2x_5 + 0.2355x_3x_4 - 0.2262x_3x_5 - 0.0117x_4x_5$
Dec	CY <sub>t-1</sub>	DA1	DA3	DA6	DA9		$29.2005 - 0.3816x_1 - 0.6953x_2 + 0.8469x_3 + 1.2024x_4 - 3.2563x_5 + 0.0005x_1^2 - 0.5339x_2^2 - 0.0047x_3^2 - 0.0119x_4^2 + 0.0083x_5^2$

493  
 494  
 495  
 496  
 497  
 498  
 499



500 **Table 5** PR models for predicting crop yield (CY) built for each month: region 2 (West Bengal). For each month,  
 501 it is indicated the input (x1 to x6) and the PR formula. DA stands for drought area.

Month	Input						PR model
	x <sub>1</sub>	x <sub>2</sub>	x <sub>3</sub>	x <sub>4</sub>	x <sub>5</sub>	x <sub>6</sub>	
Jan	CY <sub>t-1</sub>	DA3	DA6	DA9	DA12		$8.5606 - 0.2404x_1 - 1.1236x_2 - 0.7606x_3 + 6.6535x_4 - 5.3772x_5 + 0.0087x_1x_2 - 0.0044x_1x_3 - 0.0182x_1x_4 + 0.0234x_1x_5 + 0.0080x_2x_3 + 0.0234x_2x_4 - 0.0037x_2x_5 - 0.0402x_3x_4 + 0.1648x_3x_5 + 0.0200x_4x_5 + 0.0001x_1^2 - 0.0145x_2^2 - 0.0657x_3^2 + 0.0544x_4^2 - 0.0952x_5^2$
Feb	CY <sub>t-1</sub>	DA1	DA3	DA6	DA9	DA12	$-24.8742 - 0.5460x_1 - 0.1190x_2 + 0.2175x_3 + 0.7776x_4 - 8.6335x_5 + 6.4022x_6 - 0.0164x_1x_2 + 0.0095x_1x_3 - 0.0251x_1x_4 + 0.0262x_1x_5 - 0.0057x_1x_6 - 0.0179x_2x_3 - 0.0241x_2x_4 - 0.1705x_2x_5 + 0.1579x_2x_6 + 0.0064x_3x_4 + 0.2383x_3x_5 - 0.2779x_3x_6 - 0.0117x_4x_5 + 0.0266x_4x_6 + 0.0614x_5x_6$
Mar	CY <sub>t-1</sub>	DA1	DA3	DA6	DA9	DA12	$35.6904 - 0.3835x_1 - 0.9286x_2 + 0.1960x_3 - 0.3445x_4 - 0.3559x_5 + 0.6370x_6 - 0.0025x_1x_2 - 0.0009x_1x_3 + 0.0111x_1x_4 - 0.0252x_1x_5 + 0.0144x_1x_6 - 0.0059x_2x_3 + 0.0426x_2x_4 + 0.0063x_2x_5 + 0.0012x_2x_6 - 0.0362x_3x_4 - 0.1287x_3x_5 - 0.0038x_3x_6 + 0.0242x_4x_5 - 0.0355x_4x_6 + 0.0394x_5x_6$
Apr	CY <sub>t-1</sub>	DA3	DA6	DA9	DA12		$8.5856 - 0.1865x_1 + 1.5824x_2 - 1.0816x_3 - 1.0256x_4 + 1.7846x_5 - 0.0164x_1x_2 + 0.0242x_1x_3 - 0.0013x_1x_4 + 0.0009x_1x_5 - 0.0084x_2x_3 + 0.0073x_2x_4 - 0.0710x_2x_5 - 0.0430x_3x_4 + 0.0659x_3x_5 + 0.0317x_4x_5$
May	CY <sub>t-1</sub>	DA1	DA3	DA6	DA9	DA12	$-25.0101 - 0.8233x_1 - 1.8073x_2 + 1.1145x_3 + 1.6217x_4 + 0.9651x_5 + 0.5729x_6 + 0.0254x_1x_2 - 0.1198x_1x_3 + 0.0959x_1x_4 - 0.0112x_1x_5 + 0.0311x_1x_6 - 0.2178x_2x_3 + 0.3465x_2x_4 - 0.3214x_2x_5 + 0.0602x_2x_6 - 0.9192x_3x_4 + 1.2301x_3x_5 - 0.2167x_3x_6 - 0.8955x_4x_5 + 0.1015x_4x_6 + 0.0662x_5x_6 + 0.0048x_1^2 - 0.0096x_2^2 + 0.3527x_3^2 + 0.4308x_4^2 - 0.0492x_5^2 + 0.0639x_6^2$
Jun	CY <sub>t-1</sub>	DA1	DA3	DA6			$90.7623 - 0.5785x_1 + 0.1582x_2 - 2.7914x_3 + 0.8655x_4 - 0.0176x_1x_2 + 0.0093x_1x_3 - 0.0108x_1x_4 + 0.0533x_2x_3 - 0.0521x_2x_4 + 0.1589x_3x_4 + 0.0012x_1^2 + 0.0072x_2^2 - 0.0974x_3^2 - 0.0714x_4^2$
Jul	CY <sub>t-1</sub>	DA1	DA3	DA6			$26.1164 - 0.6892x_1 - 0.6723x_2 - 5.5280x_3 + 4.6922x_4 + 0.0070x_1x_2 + 0.0111x_1x_3 - 0.0148x_1x_4 - 0.1301x_2x_3 + 0.0838x_2x_4 + 0.5157x_3x_4 + 0.0014x_1^2 + 0.0679x_2^2 - 0.1671x_3^2 - 0.3540x_4^2$
Aug	CY <sub>t-1</sub>	DA1	DA3	DA6	DA9		$55.6167 - 0.2284x_1 - 0.0182x_2 - 1.7996x_3 - 4.0674x_4 + 3.7965x_5 + 0.0117x_1x_2 - 0.0259x_1x_3 + 0.0556x_1x_4 - 0.0484x_1x_5 - 0.0176x_2x_3 - 0.1459x_2x_4 + 0.1017x_2x_5 - 0.0487x_3x_4 + 0.2346x_3x_5 - 0.1273x_4x_5$
Sep	CY <sub>t-1</sub>	DA1	DA3	DA6	DA9	DA12	$35.6058 - 0.3263x_1 + 1.9755x_2 - 0.4197x_3 - 3.5963x_4 + 2.7383x_5 - 1.2234x_6 + 0.0013x_1x_2 - 0.0057x_1x_3 - 0.0470x_1x_4 + 0.0042x_1x_5 + 0.0475x_1x_6 + 0.0033x_2x_3 - 0.1889x_2x_4 + 0.0749x_2x_5 + 0.1060x_2x_6 + 0.0179x_3x_4 - 0.0003x_3x_5 + 0.0412x_3x_6 + 0.0291x_4x_5 - 0.0312x_4x_6 - 0.0379x_5x_6$
Oct	CY <sub>t-1</sub>	DA1	DA3	DA6	DA9	DA12	$7.7675 - 0.1875x_1 - 0.1476x_2 - 0.8333x_3 - 5.1327x_4 + 15.3857x_5 - 10.6323x_6 - 0.0012x_1x_2 - 0.0011x_1x_3 + 0.0588x_1x_4 + 0.0365x_1x_5 - 0.0886x_1x_6 - 0.1339x_2x_3 + 0.1763x_2x_4 - 0.5955x_2x_5 + 0.4854x_2x_6 - 0.4231x_3x_4 - 0.2159x_3x_5 + 0.6868x_3x_6 + 0.3521x_4x_5 + 0.0666x_4x_6 - 0.4145x_5x_6$
Nov	CY <sub>t-1</sub>	DA1	DA3	DA6	DA9	DA12	$38.3601 - 0.2443x_1 + 1.7236x_2 - 0.6584x_3 - 6.7484x_4 + 13.3609x_5 - 9.4895x_6 + 0.0114x_1x_2 + 0.0162x_1x_3 + 0.0331x_1x_4 - 0.0817x_1x_5 + 0.0478x_1x_6 + 0.0370x_2x_3 - 0.1350x_2x_4 - 0.0212x_2x_5 + 0.1631x_2x_6 - 0.1562x_3x_4 - 0.0082x_3x_5 + 0.1229x_3x_6 + 0.2672x_4x_5 - 0.0938x_4x_6 - 0.1335x_5x_6$
Dec	CY <sub>t-1</sub>	DA3	DA6	DA9	DA12		$24.769 - 0.1091x_1 - 2.9747x_2 + 2.9990x_3 - 5.4144x_4 + 3.3374x_5 + 0.0083x_1x_2 - 0.0069x_1x_3 + 0.0596x_1x_4 - 0.0630x_1x_5 + 0.0755x_2x_3 + 0.0127x_2x_4 + 0.0094x_2x_5 - 0.0052x_3x_4 - 0.0884x_3x_5 + 0.0361x_4x_5$

502  
 503  
 504  
 505  
 506  
 507  
 508



509 **Table 6** PR models for predicting crop yield (CY) built for each month: region 3 (Odisha). For each month, it is  
 510 indicated the input (x1 to x6) and the PR formula. DA stands for drought area.

Month	Input						PR model
	x <sub>1</sub>	x <sub>2</sub>	x <sub>3</sub>	x <sub>4</sub>	x <sub>5</sub>	x <sub>6</sub>	
Jan	CY <sub>t-1</sub>	DA3	DA6	DA9	DA12		$-149.3429 - 0.4867x_1 - 1.5749x_2 + 2.0827x_3 + 5.9761x_4 - 6.0586x_5 - 0.0022x_1x_2 + 0.0100x_1x_3 + 0.0200x_1x_4 + 0.0045x_1x_5 - 0.0142x_2x_3 - 0.2414x_2x_4 + 0.1392x_2x_5 - 0.1332x_3x_4 + 0.1123x_3x_5 + 0.2083x_4x_5 + 0.0022x_1^2 + 0.0262x_2^2 + 0.0771x_3^2 + 0.0431x_4^2 - 0.1405x_5^2$
Feb	CY <sub>t-1</sub>	DA1	DA3	DA6			$-90.6767 - 0.6674x_1 + 0.1283x_2 + 0.2580x_3 + 0.4540x_4 - 0.0041x_1x_2 + 0.0141x_1x_3 - 0.0009x_1x_4 + 0.0055x_2x_3 - 0.0195x_2x_4 + 0.0771x_3x_4 + 0.0006x_1^2 + 0.0313x_2^2 - 0.0207x_3^2 + 0.0129x_4^2$
Mar	CY <sub>t-1</sub>	DA6	DA9	DA12			$-168.6741 - 0.7249x_1 + 0.2079x_2 - 2.2594x_3 + 2.2421x_4 + 0.0074x_1x_2 - 0.0102x_1x_3 + 0.0347x_1x_4 - 0.0159x_2x_3 + 0.0009x_2x_4 + 0.1147x_3x_4 + 0.0025x_1^2 + 0.0454x_2^2 - 0.0197x_3^2 + 0.0318x_4^2$
Apr	CY <sub>t-1</sub>	DA3	DA6	DA9	DA12		$-116.7973 - 0.6789x_1 - 0.4066x_2 - 0.5459x_3 + 3.4428x_4 - 3.2126x_5 + 0.0008x_1x_2 - 0.0110x_1x_3 + 0.0063x_1x_4 + 0.0337x_1x_5 + 0.0647x_2x_3 - 0.1280x_2x_4 + 0.0847x_2x_5 - 0.0041x_3x_4 - 0.1576x_3x_5 - 0.0357x_4x_5 + 0.0025x_1^2 - 0.0386x_2^2 + 0.0180x_3^2 + 0.0968x_4^2 + 0.1431x_5^2$
May	CY <sub>t-1</sub>	DA1	DA3	DA6	DA9	DA12	$-56.0895 - 0.8435x_1 - 1.5688x_2 + 5.5848x_3 - 5.6556x_4 - 0.0876x_5 - 0.4449x_6 + 0.0396x_1x_2 - 0.0552x_1x_3 + 0.0130x_1x_4 + 0.0414x_1x_5 - 0.0155x_1x_6 + 0.0691x_2x_3 - 0.1386x_2x_4 + 0.4106x_2x_5 + 0.0874x_2x_6 + 0.2997x_3x_4 - 0.2552x_3x_5 - 0.4282x_3x_6 - 0.0482x_4x_5 + 0.2264x_4x_6 - 0.2702x_5x_6 + 0.0040x_1^2 - 0.0721x_2^2 - 0.0198x_3^2 - 0.2076x_4^2 + 0.2160x_5^2 - 0.0223x_6^2$
Jun	CY <sub>t-1</sub>	DA6	DA9	DA12			$-23.8562 - 0.3639x_1 - 1.8924x_2 - 0.0052x_3 + 1.3074x_4 - 0.0060x_1x_2 - 0.0057x_1x_3 + 0.0205x_1x_4 - 0.0135x_2x_3 - 0.0965x_2x_4 + 0.1034x_3x_4 + 0.0004x_1^2 + 0.0110x_2^2 - 0.0171x_3^2 + 0.0913x_4^2$
Jul	CY <sub>t-1</sub>	DA1	DA3	DA6	DA9	DA12	$-18.8884 - 0.7725x_1 + 2.8997x_2 - 1.9129x_3 - 0.9194x_4 - 0.5636x_5 - 0.6886x_6 - 0.0070x_1x_2 + 0.0320x_1x_3 - 0.0220x_1x_4 - 0.0221x_1x_5 - 0.0042x_1x_6 + 0.3776x_2x_3 - 0.0748x_2x_4 - 0.1803x_2x_5 - 0.2590x_2x_6 - 0.5984x_3x_4 + 0.6811x_3x_5 - 0.0178x_3x_6 + 0.8957x_4x_5 + 0.0173x_4x_6 - 0.1524x_5x_6 + 0.0012x_1^2 - 0.1151x_2^2 - 0.1006x_3^2 - 0.0306x_4^2 - 0.7603x_5^2 + 0.1200x_6^2$
Aug	CY <sub>t-1</sub>	DA1	DA3	DA6	DA9	DA12	$4.8997 - 0.7900x_1 - 0.9225x_2 + 3.8372x_3 - 0.0832x_4 - 9.7835x_5 + 4.0199x_6 - 0.0065x_1x_2 + 0.0352x_1x_3 + 0.0005x_1x_4 - 0.0461x_1x_5 - 0.0019x_1x_6 - 0.0759x_2x_3 - 0.1196x_2x_4 + 0.1775x_2x_5 + 0.0748x_2x_6 + 0.0694x_3x_4 + 0.2503x_3x_5 - 0.3715x_3x_6 - 0.2022x_4x_5 + 0.4167x_4x_6 - 0.2192x_5x_6$
Sep	CY <sub>t-1</sub>	DA1	DA3	DA6	DA9		$41.4745 - 0.5431x_1 - 0.0366x_2 - 0.9681x_3 + 3.6023x_4 - 4.3272x_5 - 0.0002x_1x_2 + 0.0115x_1x_3 - 0.0191x_1x_4 + 0.0139x_1x_5 - 0.0809x_2x_3 + 0.0508x_2x_4 + 0.0205x_2x_5 + 0.4602x_3x_4 - 0.5016x_3x_5 + 0.3000x_4x_5 + 0.0002x_1^2 + 0.0172x_2^2 - 0.0339x_3^2 - 0.3409x_4^2 + 0.0831x_5^2$
Oct	CY <sub>t-1</sub>	DA1	DA3	DA6			$-48.806 - 0.6966x_1 - 0.4241x_2 - 1.7664x_3 - 3.0097x_4 + 0.0040x_1x_2 + 0.0053x_1x_3 - 0.0175x_1x_4 - 0.0038x_2x_3 + 0.0111x_2x_4 - 0.1443x_3x_4 + 0.0008x_1^2 + 0.0073x_2^2 + 0.0861x_3^2 + 0.0558x_4^2$
Nov	CY <sub>t-1</sub>	DA1	DA3	DA6			$47.8316 - 0.6925x_1 + 0.7765x_2 - 2.3671x_3 - 2.9813x_4 + 0.0043x_1x_2 + 0.0011x_1x_3 - 0.0066x_1x_4 + 0.0797x_2x_3 - 0.0306x_2x_4 - 0.0144x_3x_4 + 0.0004x_1^2 - 0.0064x_2^2 - 0.0407x_3^2 + 0.0200x_4^2$
Dec	CY <sub>t-1</sub>	DA6	DA9				$13.0378 - 0.5111x_1 + 0.5765x_2 - 3.4820x_3 + 0.0177x_1x_2 - 0.0158x_1x_3 + 0.0155x_2x_3 + 0.0004x_1^2 - 0.0691x_2^2 + 0.0343x_3^2$

511

512 **4.5 ML modelling limitations**

513 The limitations of the presented approach are the following.

- 514 (1) To determine drought areas, a threshold value of the Standardised Precipitation  
 515 Evapotranspiration Index (SPEI) drought index ( $SPEI \leq -1$ ) was used. Using just one threshold  
 516 might lead to over or underestimation of the actual drought impacts over crop yield.



517 (2) Gridded data of SPEI at spatial resolution ( $0.5^{\circ} \times 0.5^{\circ}$ ) was used in this study over each  
518 region individually. Using such a coarse spatial resolution on different region sizes might not  
519 capture the drought area correctly, leading to over or underestimating its magnitude.

520 (3) The study area has a diverse ecosystem of irrigated and rain-fed land, which may influence  
521 the correlation between DA and crop yield more or less.

522 (4) This study assumes that drought is the only causative factor; however, floods negatively  
523 impact crop yield in the region, thus in the total production in the regions. Flood impacts are  
524 not considered in the models.

525 (5) Many other factors might influence rice yield, such as market, technologies, management,  
526 etc. In this study, it was assumed that drought plays the prominent role.

527 (6) Insufficient crop yield data for the ML model building was an issue because the CY time  
528 series only had one value for each year.

## 529 **5 Summary and conclusions**

530 This research introduced a step-by-step ML approach for predicting crop yield (CY) with  
531 drought areas (DAs) as input. The ML approach comprises two components. Each component  
532 employs two types of ML models: polynomial regression (PR) and artificial neural network  
533 (ANN). The goal was to build the ML models (ANN and PR) and use them as an integrated  
534 tool to crop yield prediction. The formulas of the PR models were also provided. The ML  
535 approach was applied in three East India regions.

536 The following conclusions are drawn from this research.

- 537 • Based on the performance of PR and ANN models, results show drought area to be a  
538 suitable variable to predict crop yield.
- 539 • The correlation analysis between DA and CY showed high negative correlations in  
540 Odisha (region 3). The correlation gradually decreases in Bihar and Jharkhand (region  
541 1) and West Bengal (region 2). These correlation values can be because West Bengal  
542 has better access to irrigation facilities than Odisha and Bihar & Jharkhand.
- 543 • On comparing ANN models and PR models, the ANN were more accurate than PR  
544 models to predict crop yield for all regions. This could have been expected since the  
545 drought–crop relationship is a highly non-linear problem.
- 546 • It can be concluded that ANN has a high capability to predict CY in the pre-harvesting  
547 stage with good accuracy, considering the drought indicator used (SPEI), which uses  
548 climate variables such as precipitation and temperature (for evapotranspiration  
549 calculation).



550 From the analysis and findings of this research, the following recommendations can be  
551 provided for further improvement.

- 552 • Sensitivity analysis should be performed to identify the parameters that can impact the  
553 model results. For instance, different spatial resolutions of drought indicator and  
554 different thresholds should be investigated.
- 555 • Wet extreme events should be considered, especially in the flood-prone regions such as  
556 the coastal areas of West Bengal (region 2) and Odisha (region 3) and North Bihar  
557 (region 1), where floods also influence crop yield.
- 558 • Non-climatic factors such as econometric, fertilisers, and management practices might  
559 be considered because they influence crop yield.
- 560 • In order to improve the model accuracy, more input data should be used in further  
561 studies. For CY, this can be estimated by remote sensing techniques on a monthly basis  
562 so that the ML models can be built for this temporal resolution and the spatial coverage  
563 can be better addressed.
- 564 • The performance of other ML models has to be investigated, especially committee  
565 (ensemble) methods like random forests or boosting methods. In the case of data at  
566 scales less than monthly, the use of deep learning algorithms (e.g. LSTM networks)  
567 could be recommended to explore.

568 We envision that this research will improve drought monitoring systems for assessing drought  
569 effects. Since it is currently possible to calculate drought areas within these systems, the direct  
570 application of the prediction of drought effects is possible to integrate by following approaches  
571 such as the one presented or similar.

## 572 **Coda and data availability**

573 State-wise crop-yield data was retrieved through the Indian Directorate of Economic and Statistics from the  
574 Department of Agriculture (DAC) (<http://eands.dacnet.nic.in/>). The SPEI data was retrieved from the SPEI Global  
575 Drought Monitor (<https://spei.csic.es>). The code is available upon request from the corresponding author.

## 576 **Competing interests**

577 An author is member of the editorial board of journal HESS. The peer-review process was guided by an  
578 independent editor, and the authors have also no other competing interests to declare.

## 579 **Acknowledgements**

580 VD thanks the Mexican National Council for Science and Technology (CONACYT) and Alianza FiiDEM for the  
581 study grand 217776/382365. AAAO was supported by the Orange Knowledge Programme (former NFP) and the  
582 World Meteorological Organization (WMO). GACP and VD acknowledge the grand No. 2579 of the Prince  
583 Albert II of Monaco Foundation. HvL is supported by the H2020 ANYWHERE project (Grant Agreement No.  
584 700099). DS acknowledges the grant No. 17-77-30006 of the Russian Science Foundation, and the  
585 Hydroinformatics research fund of IHE Delft in whose framework some research ideas and components were  
586 developed. The study is also a contribution to the UNESCO IHP-VII programme (Euro FRIEND-Water project)  
587 and the Panta Rhei Initiative on Drought in the Antropocene of the International Association of Hydrological  
588 Sciences (IAHS).



589 **References**

- 590 Below, R., Grover-Kopec, E., and Dilley, M. (2007). Documenting Drought-Related Disasters:  
591 A Global Reassessment. *J. Environ. Dev.*, 16(3), 328–344.  
592 <https://doi.org/10.1177/1070496507306222>
- 593 Bhalme, H.N. and Mooley, D. a. (1980). Large-Scale Droughts/Floods and Monsoon  
594 Circulation. *Monthly Weather Review*, 108(8), 1197–1211. [https://doi.org/10.1175/1520-0493\(1980\)108<1197:LSDAMC>2.0.CO;2](https://doi.org/10.1175/1520-0493(1980)108<1197:LSDAMC>2.0.CO;2)
- 596 Chlingaryan, A., Sukkarieh, S., and Whelan, B. (2018). Machine learning approaches for crop  
597 yield prediction and nitrogen status estimation in precision agriculture: A review.  
598 *Computers and Electronics in Agriculture*, 151(May), 61–69.  
599 <https://doi.org/10.1016/j.compag.2018.05.012>
- 600 Corzo Perez, G.A., van Huijgevoort, M.H.J., Voß, F., and van Lanen, H.A.J. (2011). On the  
601 spatio-temporal analysis of hydrological droughts from global hydrological models.  
602 *Hydrology and Earth System Sciences*, 15(9), 2963–2978. <https://doi.org/10.5194/hess-15-2963-2011>
- 604 Dai, A. (2011). Characteristics and trends in various forms of the Palmer Drought Severity  
605 Index during 1900 – 2008. *Journal of Geophysical Research*, 116(March), 1–26.  
606 <https://doi.org/10.1029/2010JD015541>
- 607 Diaz, V., Corzo, G., Van Lanen, H.A.J., and Solomatine, D.P. (2019). Spatiotemporal Drought  
608 Analysis at Country Scale Through the Application of the STAND Toolbox.  
609 *Spatiotemporal Analysis of Extreme Hydrological Events*, 77–93.  
610 <https://doi.org/10.1016/B978-0-12-811689-0.00004-5>
- 611 Diaz, V., Corzo Perez, G.A., Van Lanen, H.A.J., Solomatine, D., and Varouchakis, E.A.  
612 (2020). An approach to characterise spatio-temporal drought dynamics. *Advances in*  
613 *Water Resources*, 137, 103512.  
614 <https://doi.org/https://doi.org/10.1016/j.advwatres.2020.103512>
- 615 Elshorbagy, A., Corzo, G., Srinivasulu, S., and Solomatine, D.P. (2010). Experimental  
616 investigation of the predictive capabilities of data driven modeling techniques in  
617 hydrology - Part 2: Application. *Hydrology and Earth System Sciences*, 14(10), 1943–  
618 1961. <https://doi.org/10.5194/hess-14-1943-2010>
- 619 Food and Agriculture Organization of the United Nations (FAO). (2017). *The Impact of*  
620 *disasters and crises on agriculture and Food Security*. Retrieved from  
621 [www.fao.org/publications](http://www.fao.org/publications)



- 622 Food and Agriculture Organization of the United Nations (FAO) and Robert B Daugherty  
623 Water for Food Institute at the University of Nebraska. (2015). *Yield gap analysis of field*  
624 *crops, Methods and case studies*. (V. O. Sadras, K. G. G. Cassman, P. Grassini, A. J. Hall,  
625 W. G. M. Bastiaanssen, A. G. Laborte, ... P. Steduto, Eds.), *FAO Water Reports* (Vol.  
626 41). Rome, Italy.
- 627 Ghosh, K., Balasubramanian, R., Bandopadhyay, S., Chattopadhyay, N., Singh, K.K., and  
628 Rathore, L.S. (2014). Development of crop yield forecast models under FASAL—a case  
629 study of kharif rice in West Bengal. *Journal of Agrometeorology*, *16*(1), 1–8.
- 630 Govindaraju, R.S. (2000). Artificial Neural Networks in Hydrology. I: Preliminary Concepts.  
631 *Journal of Hydrologic Engineering*, *5*(2), 115–123. [https://doi.org/10.1061/\(ASCE\)1084-](https://doi.org/10.1061/(ASCE)1084-0699(2000)5:2(115))  
632 [0699\(2000\)5:2\(115\)](https://doi.org/10.1061/(ASCE)1084-0699(2000)5:2(115))
- 633 Guha-Sapir, D. (2019). EM-DAT: The Emergency Events Database - Université catholique de  
634 Louvain (UCL) - CRED. Retrieved from [www.emdat.be](http://www.emdat.be)
- 635 Herrera-Estrada, J.E., Satoh, Y., and Sheffield, J. (2017). Spatio-Temporal Dynamics of Global  
636 Drought. *Geophysical Research Letters*, *44*, 2254–2263.  
637 <https://doi.org/10.1002/2016GL071768>
- 638 Huang, J., Gómez-Dans, J.L., Huang, H., Ma, H., Wu, Q., Lewis, P.E., Liang, S., Chen, Z.,  
639 Xue, J.H., Wu, Y., Zhao, F., Wang, J., and Xie, X. (2019). Assimilation of remote sensing  
640 into crop growth models: Current status and perspectives. *Agricultural and Forest*  
641 *Meteorology*, *276–277*(July), 107609. <https://doi.org/10.1016/j.agrformet.2019.06.008>
- 642 Kim, W., Iizumi, T., and Nishimori, M. (2019). Global Patterns of Crop Production Losses  
643 Associated with Droughts from 1983 to 2009. *Journal of Applied Meteorology and*  
644 *Climatology*, *58*(6), 1233–1244. <https://doi.org/10.1175/JAMC-D-18-0174.1>
- 645 Maier, H.R. and Dandy, G.C. (2000). Neural networks for the prediction and forecasting of  
646 water resources variables: a review of modelling issues and applications. *Environmental*  
647 *Modelling & Software*, *15*(1), 101–124. [https://doi.org/10.1016/S1364-8152\(99\)00007-9](https://doi.org/10.1016/S1364-8152(99)00007-9)
- 648 May, R., Dandy, G., and Maier, H. (2011). Review of Input Variable Selection Methods for  
649 Artificial Neural Networks. In G. Dandy (Ed.), *Artificial Neural Networks -*  
650 *Methodological Advances and Biomedical Applications* (p. Ch. 2). Rijeka: InTech.  
651 <https://doi.org/10.5772/16004>
- 652 Mckee, T.B., Doesken, N.J., and Kleist, J. (1993). The relationship of drought frequency and  
653 duration to time scales. *AMS 8th Conf. Appl. Climatol.*, (January), 179–184.  
654 <https://doi.org/citeulike-article-id:10490403>
- 655 Monfreda, C., Ramankutty, N., and Foley, J.A. (2008). Farming the planet: 2. Geographic



- 656 distribution of crop areas, yields, physiological types, and net primary production in the  
657 year 2000. *Global Biogeochem. Cycles*, 22(1), 1–19.  
658 <https://doi.org/10.1029/2007GB002947>
- 659 Montesino Pouzols, F. and Lendasse, A. (2010). Effect of different detrending approaches on  
660 computational intelligence models of time series. In *The 2010 International Joint*  
661 *Conference on Neural Networks (IJCNN)* (pp. 1–8). IEEE.  
662 <https://doi.org/10.1109/IJCNN.2010.5596314>
- 663 Naresh Kumar, M., Murthy, C.S., Sessa Sai, M.V.R., and Roy, P.S. (2012). Spatiotemporal  
664 analysis of meteorological drought variability in the Indian region using standardized  
665 precipitation index. *Meteorological Applications*, 19(2), 256–264.  
666 <https://doi.org/10.1002/met.277>
- 667 Rahmati, O., Falah, F., Dayal, K.S., Deo, R.C., Mohammadi, F., Biggs, T., Moghaddam, D.D.,  
668 Naghibi, S.A., and Bui, D.T. (2020). Machine learning approaches for spatial modeling  
669 of agricultural droughts in the south-east region of Queensland Australia. *Science of the*  
670 *Total Environment*, 699, 134230. <https://doi.org/10.1016/j.scitotenv.2019.134230>
- 671 Reynolds, C.A., Yitayew, M., Slack, D.C., Hutchinson, C.F., Huete, A., and Petersen, M.S.  
672 (2000). Estimating crop yields and production by integrating the FAO Crop Specific  
673 Water Balance model with real-time satellite data and ground-based ancillary data.  
674 *International Journal of Remote Sensing*, 21(18), 3487–3508.  
675 <https://doi.org/10.1080/014311600750037516>
- 676 Sawasawa, H. (2003). *Crop yield estimation: Integrating RS, GIS and management factors, a*  
677 *case study of Birkoor and Kortigiri Mandals. MSc thesis*. International Institute for Geo-  
678 information Science and Earth Observation. Retrieved from  
679 [http://www.itc.nl/library/papers\\_2003/msc/nrm/sawasawa.pdf](http://www.itc.nl/library/papers_2003/msc/nrm/sawasawa.pdf)
- 680 Sheffield, J. and Wood, E.F. (2011). *Drought: Past problems and future scenarios*. (P.  
681 Earthscan, Ed.). London.
- 682 Udmale, P., Ichikawa, Y., Ning, S., Shrestha, S., and Pal, I. (2020). A statistical approach  
683 towards defining national-scale meteorological droughts in India using crop data.  
684 *Environmental Research Letters*, 15(9). <https://doi.org/10.1088/1748-9326/abacfa>
- 685 van Klompenburg, T., Kassahun, A., and Catal, C. (2020). Crop yield prediction using machine  
686 learning: A systematic literature review. *Computers and Electronics in Agriculture*,  
687 177(July), 105709. <https://doi.org/10.1016/j.compag.2020.105709>
- 688 White, M.A., Thornton, P.E., and Running, S.W. (1997). A continental phenology model for  
689 monitoring vegetation responses to interannual climatic variability. *Global*





- 690 *Biogeochemical Cycles*, 11(2), 217–234. <https://doi.org/10.1029/97GB00330>
- 691 World Meteorological Organization (WMO). (2006). *Drought monitoring and early warning:*  
692 *concepts, progress and future challenges*. WMO-No. 1006. Geneva, Switzerland.  
693 Retrieved from  
694 [http://www.droughtmanagement.info/literature/WMO\\_drought\\_monitoring\\_early\\_warni](http://www.droughtmanagement.info/literature/WMO_drought_monitoring_early_warning_2006.pdf)  
695 [ng\\_2006.pdf](http://www.droughtmanagement.info/literature/WMO_drought_monitoring_early_warning_2006.pdf)
- 696 Wu, X., Vuichard, N., Ciais, P., Viovy, N., Wang, X., Magliulo, V., and Wattenbach, M.  
697 (2016). ORCHIDEE-CROP (v0), a new process-based agro-land surface model: model  
698 description and evaluation over Europe, 857–873. [https://doi.org/10.5194/gmd-9-857-](https://doi.org/10.5194/gmd-9-857-2016)  
699 2016  
700